
**UNIVERSITA' DI PISA**
**Facolta' di Farmacia**
Corso di Laurea Specialistica in Farmacia

# *Novel indole derivatives as candidates for the development of molecolar probes for TSPO*

**Relatori:**

Dott.ssa Sabrina Taliani
Dott.ssa Elisabetta Barresi

**Candidato:**

Carmassi Giulia

Anno Accademico 2011/2012

*A mia madre*

# INDEX

# INTRODUCTION

Benzodiazepines (BZs), such as diazepam and chlordiazepoxide, are safe drugs used to controlled anxiety and sleep disorders.[1] They have got two different types of receptors called: **central benzodiazepine receptors (CBRs)** and **peripheral benzodiazepine receptors (PBRs)**.

- ***CBRs*** is present in the brain and forms an allosteric site on the $GABA_A$ receptor complex. Some ligands acting at this allosteric site, as well as, diazepam and chlordiazepoxide, enhance the affinity of the γ-aminobutyric acid (GABA) toward the CBR and, in this way, influence chloride ($Cl^-$) influx at the $GABA_A$ receptor pore, causing downstream effects on GABA-mediated inhibition.[2]
  Other studies have shown benzodiazepines (BZs) acting on CBRs to be responsible for different $GABA_A$-induced effects: BZs are used clinically as muscle relaxants, anticonvulsants, anxiolytics and sedative-hypnotics.[2] This drugs have got numerous collateral effects, for example: ethanol potentiation, amnesia, ataxia, dizziness and the risk of dependence if used for too time.[1]

- **PBRs** is first described by Braestrup and Squires[4] in 1977, as an alternative binding site in non-neuronal tissue for the diazepam, a centrally acting benzodiazepine. It was named *peripheral* according to this tissue distribution and *benzodiazepine receptor* because BZs is the class of ligands by which PBR was discovered. Other names have been used to refer to this protein, including *mitochondrial benzodiazepine receptor (MBR), mitochondrial diazepam binding inhibitor (DBI) receptor complex (mDRC), PK11195 binding sites (PKBs), isoquinoline binding protein (IBP), Omega3 (*ω3*) receptor.* [5]

Although the name PBR was much used in the scientific community, in 1996 it change in the new name **Translocator Protein 18 kDa**, abbreviated **TSPO**, proposed by Papadopoulos and colleagues[6] because it didn't take into account the new findings regarding its structure, subcellular roles and tissue distribution. It has also been shown that many ligands structurally different from BZs bind to this protein, which is not a very receptor in the traditional sense, but rather a translocator of molecules as well as cholesterol and protoporphyrins. In this thesis work is adopted the abbreviation TSPO instead of PBR.

Braestrup and Squires [4] during their pharmacological studies, noticed a specific binding of [$^3$H] diazepam to receptors in rat kidney, liver and lung, but at the same time observed that binding in non-neuronal tissue appeared to be very different from the specific binding to brain membranes: first, while binding in kidney was associated with mitochondrial fraction, in brain it was associated with a membrane fraction; second, the affinity for receptors in kidney was lower than that for brain binding sites.
In 1982 Marangos et al. confirmed that TSPO has a brain regional distribution distinct from that of CBR and that it is not linked to GABA-regulated anion channels.[7] Receptor binding was assayed using diazepam, that has got high affinity to CBR and weakly with

TSPO and the Ro 5-4864 (7-chloro-1,3-dihydro-1-methyl-5-(p-chlorophenyl)-2H-1,4-benzodiazepine-2-one), which differs from diazepam only by a chloride in the 5' aromatic ring and that has a nanomolar affinity for TSPO (7.3nM) [8] but a very low affinity for $GABA_A$ receptors (163 μM[9] in rat brain membranes) (**Figure 1**).

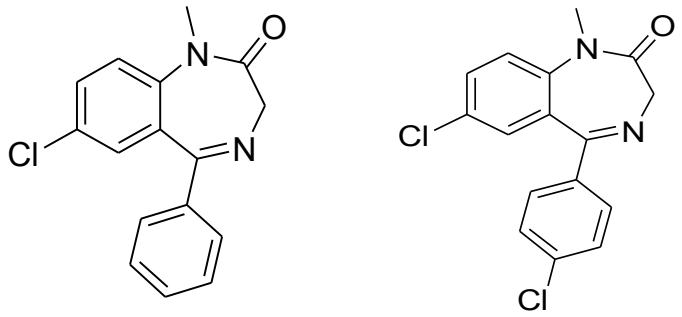


Diazepam (**1**) Ro 5-4864 (**2**)

**Figure 1**. Diazepam (**1**) and Ro 5-4864 (**2**)

Following studies have determined the high mitochondrial localization of TSPO and the smaller concentration in some subcellular compartments as well as plasma membrane, lysosomes, peroxisomes, nuclei and Golgi apparatus.
In 1986 Anholt and co-workers investigated the submitochondrial localization of TSPO, using cytochrome oxidase as marker for the inner membrane and monoamine oxidase as outer membrane marker. Treating rat adrenal mitochondria with digitonin, a detergent able to separate the outer membrane from the inner membrane, they noticed that the release of TSPO increased parallel to the release of monoamine oxidase and provided evidence for the association of TSPO with the mitochondrial outer membrane.[10]
Following studies have determined that TSPO is very concentrated in a particular sites called **mitochondrial permeability transition pore** abbreviated **MPTP** and exactly at contact sites between the outer/inner mitochondrial membranes.[11]

# Structure of TSPO

TSPO is a protein with a molecular mass of 18 kDa, that was identified in 1988 by Antkiewicz-Michaluk et al.[12] using photolabeling studies, from the rat adrenal gland. It is a very hydrophobic and tryptophan-rich protein of 169 amino acids highly conserved throughout species. Three-dimensional modeling has revealed a structure with five transmembrane domains consisting of α-helices composed of 21 residues that span the entire membrane bilayer, with a carboxyl-terminal tail located outside the mitochondria and an amino terminal inside the mitochondria [13,14] (**Figure 2**). Following, topographic studies have demostrate that the 18 kDa TSPO protein is organized in clusters of four to six molecules to form a single pore, reflecting the recognized function of transporter in the mitochondrial membrane.[15]

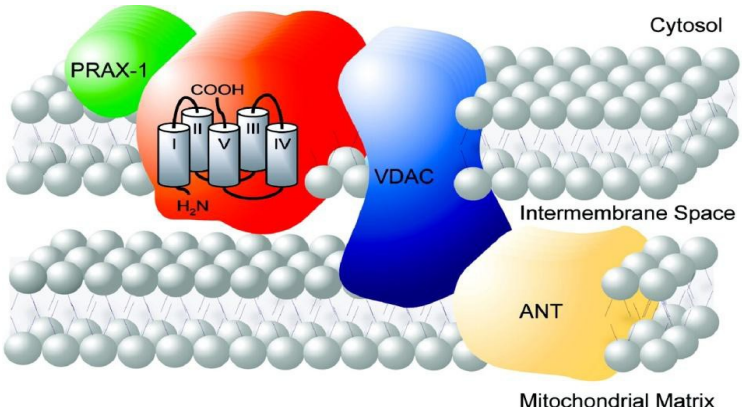


**Figure 2**. Molecular structure of 18kDa TSPO and localization at the contact site between the outer and inner mitochondrial membrane. It is also shown some proteins associated with TSPO in the MPTP complex (VDAC, ANT and PRAX-1).[13]

McEnery et al. in 1992 discovered that TSPO is strictly associated in a trimeric complex with :

- **ANT**, **adenine nucleotide translocase**, a specific antiporter of 30 kDa, located in the inner mitochondrial membrane, for the exchange of ATP and ADP as part of oxidative phosphorylation.

- **VDAC**, **a voltage-dependent anion channel** of 32 kDa located at sites of contact between outer and inner mitochondrial membrane that acting as a channel allowing passage of small molecules and ions into the mitochondria.[13,14] These three subunits constitute together with other proteins, the mitochondrial permeability transition pore, abbreviated MPTP. [16]

There are four cytosolic TSPO-associated proteins which most of time play an important role in the biological processes where TSPO is involved:

- **p10** is the first cytosolic protein associated to TSPO identified, but whose

biochemical role has not been understood yet. It is a protein of 10 kDa that coimmunoprecipited with 18 kDa TSPO using the isoquinoline carboxamide radioactive probe PK14105, a ligand selective for mitochondrial benzodiazepine receptors, to photolabel rat mitochondrial preparations. [17]

- **PKA-associated protein 7 (PAP7)** is a cytosolic protein with a molecular mass of 52 kDa involved in the hormonal regulation of steroid formation, interacting with both the cytosolic RIα subunit of PKA and TSPO. Particularly, PAP7 targets the PKA isoenzyme, linked to increased steroid synthesis, which phosphorylating specific protein substrates induces the reorganization of TSPO topography and function. [20]

- **Steroidogenic Acute Regulatory Protein (StAR),** that mediates the flow of cholesterol from the outer to the inner mitochondrial membrane, permitting steroid formation in steroidogenic cell. Following studies indicated that StAR acts at the outer mitochondrial membrane and it is not needed to allowed the entry of cholesterol into mitochondria. Therefore, Hauet et al. suggest that TSPO and StAR work in concert to bring cholesterol into mitochondria and in particular TSPO serves as a gatekeeper in cholesterol import into mitochondria and StAR plays the role of the hormone-induced activator. [19,20]

- ***PBR associated protein-1 (PRAX-1)*** is isolated, cloning and characterized by Galiègue et al. in 1999. [21] It is a protein of 1857 amino acids with a molecular mass of 240 kDa, discovered using the yeast two-hybrid screening strategy. Exhibiting various domains involved in protein-protein interaction, such as proline-rich domains, leucine-zipper motifs and Src homology region 3-like (SH3-like) dodomains, it has been suggested that PRAX-1 acts as an adaptor protein to recruit additional targets to the vicinity of TSPO so as to modulate its function. In addition, it was assumed that a single PRAX-1 protein interacts with the C-terminal end (14 amino acids) of several molecules of TSPO (at least two of them) (**Figure 3**).

**Figure 3.** Hypothetical model of the interaction between TSPO and PRAX-1.[21]

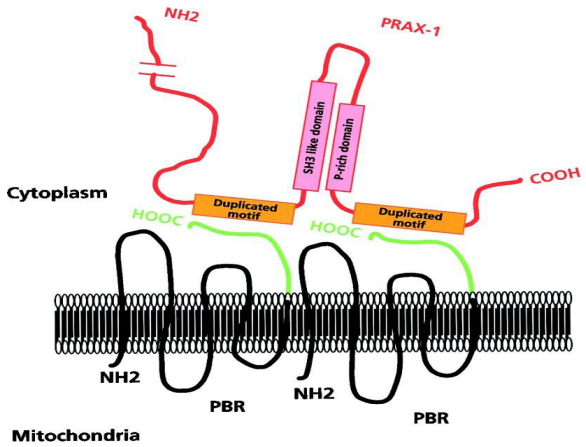

# Distribution of TSPO

The expression of TSPO is ubiquitary, although it considerably varies among tissues, for example is different between peripheral tissues and *central nervous system (CNS)*. An high density of TSPO is found in secretory and glandular tissues, such as adrenal glands, pineal glands, salivary glands, olfactory epithelium, ependyma and gonads, therefore in steroid producing tissues. Intermediate levels of TSPO are detected in renal and myocardial tissues; in contrast, the brain (in particular glia, microglia and reactive astrocytes) and liver express in normal condition relatively low levels of this protein. TSPO are also found among all human peripheral blood leukocyte subsets, particularly in monocytes, polymorphonuclear cells and lymphocytes, and in mature human erythrocytes.[14]
Other example of periperal tissues in with TSPO is present are: heart, liver, kidney, immune system and lung.[5]
TSPO density can be modulated under a variety of physiological or pathological conditions. In fact, TSPO is generally highly expressed in steroidogenic cells such as testicular and adrenocortical cells; elevated levels of TSPO, compared to healthy human tissues, have also been detected in cancerous tissues of the breast, ovary, colon, prostate, and brain glial tumor cells. It has also been supposed a correlation between TSPO levels and the metastatic potential of human breast cancer and brain gliomas.[22]
TSPO is upregulated in brain injury and inflammation, in various neuropathological conditions (certain types of epilepsy, stroke, herpes and HIV encephalitis) and neurodegenerative disorders (Alzheimer's disease, multiple sclerosis, amyotrophic lateral sclerosis, Parkinson's disease and Huntington's disease). Moreover, TSPO levels are decreased in patients with generalized anxiety (detected in lymphocytes and platelets), panic, post-traumatic stress and obsessive-compulsive disorders. Changes in TSPO expression have been observed during ischemia-reperfusion injury, indicating a role for TSPO in maintaining kidney function and renal protection. [19, 22, 23]

# Functions of TSPO

TSPO is involved in numerous biological processes as well as regulation of immune functions, cholesterol transport, lipid metabolism, steroidogenesis, calcium homeostasis, cell growth and differentiation mitochondrial oxidation and regulation of immune functions. [14,24]

- **IMMUNOMODULATION:** TSPO has got an important role in host defense mechanisms and inflammatory response. It is expressed in a numerous cells involved in the regulation of the immune responses as well as microglia, blood monocytes and leukocytes. Some TSPO ligands, mainly benzodiazepines, have an immunosuppressive action, inhibiting the capacity of macrophages to produce ROS (*reactive oxygen species*) and inflammatory cytokines as well as IL-1 (*interleukin-1*), TNFα (*tumor necrosis factor alpha*) and IL-6, and regulating phagocyte oxidative metabolism required for elimination of foreign antigens.[16] Furthermore, this antiinflammatory action TSPO-mediated is also due to its capacity of stimulate glucocorticoid synthesis in steroidogenic organs and in local tissue damage.[5]
  TSPO is mainy expressed in CNS in microglia and in astrocytes.
  Several studies have demonstrated that under conditions resulting in glialactivation, as well as inflammation and metabolic stress, basal levels of TSPO in these cells can increase in a time-dependent manner. This up-regulation of TSPO has been observed in traumatic, ischemic and chemically-induced brain injury, in neurodegenerative disorders, i.e., in the temporal cortex from patients with Alzheimer's disease and Huntington's disease, in the epilepsy, multiple sclerosis and experimental autoimmune encephalomyelitis.[14]
  Activation of microglia consists in migration to the site of damage, proliferation, production and release of potent neuroinflammatory cytokines (TNFα, IL-1β), arachidonic acid derivatives as well as cyclooxygenase-2,excitatory amino acids, and ROS. As inflammatory responses mediated by the activation of microglia may aggravate in neuronal damage, and TSPO has proved to be a promising marker for activated microglia, it has attempted to develop specific TSPO ligands able to prevent or limit neuroinflammation or to label the same activated microglia to track the progression of neuroinflammation.[16]

- **APOPTOSIS:** MPTP plays an important role in the modulation of signaling pathways mediating apoptotic and necrotic cell death.
  The exact composition of the MPTP is not yet established, but it has been recognized various proteins implicated in pore formation and its regulation (**Figure 4**): an hexokinase, in the cytosol; a trimeric complex constituted by VDAC, ANC and TSPO; a creatine kinase in the intermembrane space and cyclophilin D in the matrix.

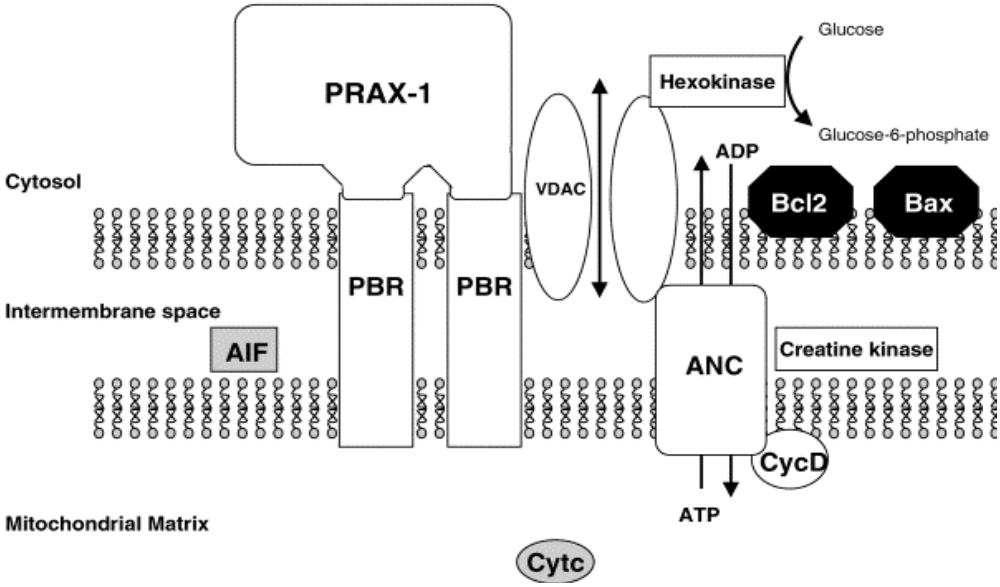


**Figure 4.** Schematic structure of the MPTP.[14]

MPTP allows the transfer of solutes, including ATP/ADP exchange, from the mitochondrial matrix to cytosol, through the VDAC/ANC conduit, and therefore facilitates the crossing of the highly impermeable mitochondrial inner membrane. This periodic transient increase in permeability by the MPTP allows the pumping of protons from the inner membrane by the electron transport chain and creates the transmembrane electrochemical gradient that drives ATP synthesis. [14, 16]

Other factors cause the opening of the MPTP: high [$Ca^{2+}$], low adenine nucleotide concentrations, high phosphate concentrations, oxidative stress and pro-apoptotic proteins as well as Bcl-2. Pore opening leads to the dissipation of transmembrane electrochemical gradient, uncoupling of mitochondria and swelling, resulting in the release of *cytochrome c* and *apoptosis inducing factor (AIF)* into the cytosol. Once in the cytosol, the first induces the caspase cascade ending in the destruction of cell nucleus, cytoskeleton and plasma membrane; the second principally leads to nuclear chromatin condensation, DNA fragmentation and then to cell death.[14]

TSPO is an endogenous modulator of apoptotic process but the exact molecular events involved have not yet been definitively clarified. There are two different types of possible mechanisms for regulating the apoptotic pathway by TSPO. One of this is illustrated in **Figure 5**. The first types of this mechanisms was supposed in 2008 by Veenman et al. [26] They suggested that interaction between VDAC and TSPO is fundamental to initiate the mitochondrial apoptosis pathway. The intermediary agent between TSPO and VDAC was supposed to be provided by mitochondrial *ROS* generation under the control of the same TSPO. ROS lead first to dissociation of *cytochrome c* from oxidized cardiolipins located at the inner mitochondrial membrane and, subsequently to its release in the cytosol via formation of a pore due to assemblage of VDAC molecules.

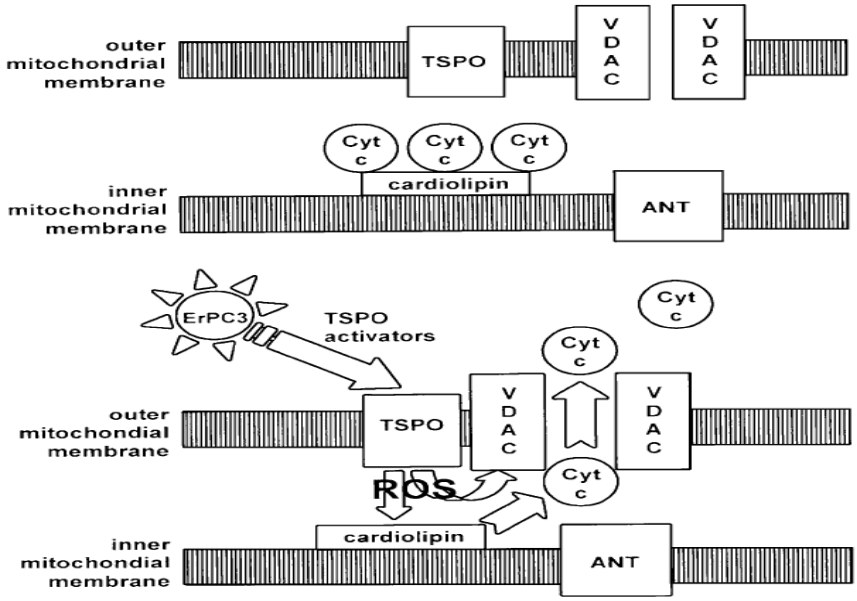


**Figura 5.** TSPO regulation of the mitochondrial apoptosois pathway. [26]

Another possible mechanism was proposed in 2007 by Azarashvili et al.[27] that provided evidence for TSPO involvement in MPTP opening, controlling the $Ca^{2+}$-induced $Ca^{2+}$ efflux and AIF release from mitochondria, important stage of initiation of programmed cell death.
It has also been observed a modulation by TSPO of interactions between VDAC or ANT and pro-apoptotic (Bcl-2) or anti-apoptotic proteins (Bax). [28]
Therefore, it has been designed TSPO ligands with pro-apoptotic effects acting as anticancer agents. In 2005 Chelli et al.[30] proposed PIGA, a ligand chosen from the *N,N*-dialkyl-2-phenylindol-3-ylglyoxylamide series, as a novel pro-apoptotic compound with therapeutic potential against glial tumours. TSPO-binding ligands have also been widely explored as carrier for receptor-mediated drug delivery, as well as TSPO ligand-Ara-C conjugates[30] and Pt complexes.[31]

- **STEROIDOGENESIS:** The most extensively characterized function of TSPO concerns its role in steroid biosynthesis. Two important observations suggest that TSPO plays an important role in steroidogenesis: first, the location of this protein on the outer mitochondrial membrane and second, the extremely high density in steroidogenic endocrine tissues, as well as adrenocortical cells and Leydig cells. Different publications report that TSPO ligands stimulate steroid biosynthesis in adrenal, placental, testicular, ovarian and glial systems. [32, 33]
  The biosynthesis of steroids begins with the enzymatic transformation of cholesterol into pregnenolone, which occurs through cholesterol side-chain cleavage by the *cytochrome P450scc* (also known as CYP11A1) and auxiliary electron transferring proteins, localized on the matrix side of the inner mitochondrial membrane (**Figure 6**). Pregnenolone then leaves mitochondria to move to the endoplasmic reticulum, where it is transformed in the final steroid products. [6, 16, 19]

The rate-limiting step is the translocation of cholesterol from the cellular stores across the aqueous intermembrane space to the inner mitochondrial membrane and *P450scc* (*cytochrome P450 side-chain cleavage*).

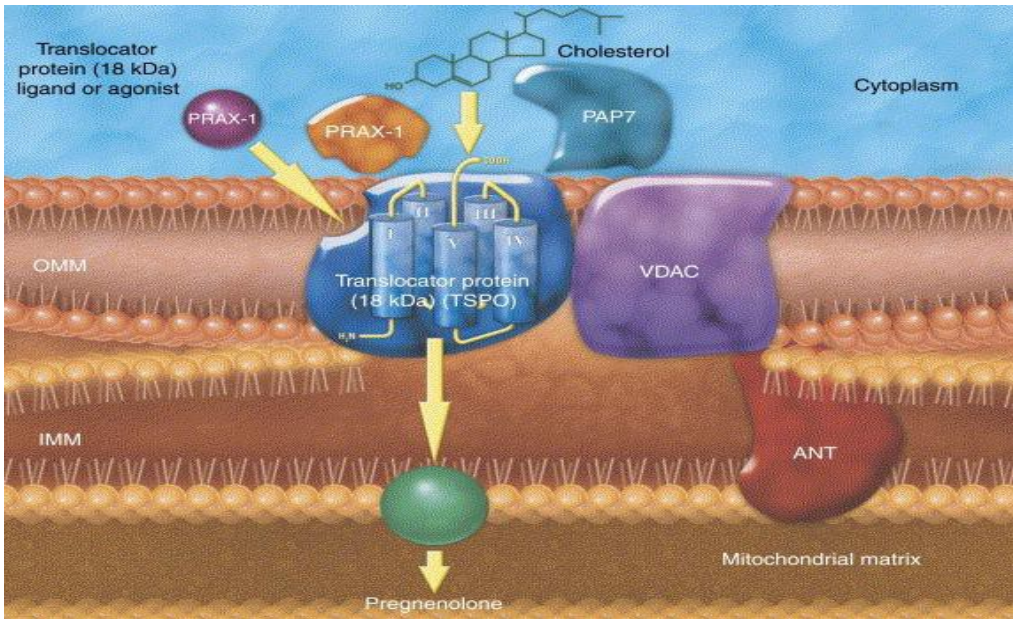


**Figura 6.** TSPO facilitating mitochondrial cholesterol delivery regulates the synthesis of steroids.[6]

Knockout and antisense experiments in vitro have demonstrated that down-regulation of TSPO causes a decrease in steroid synthesis. [16, 32, 33]

The topographic study of TSPO in the mitochondrial membranes have also shown that after treatment of Leydig cells with a steroidogenesis stimulator, as well as choriogonadotrophin hormone (hCG), there are various morphological changes, for example a formation of large complexes of 15-25 molecules of TSPO and a rapid reorganization of their localization in the mitochondrial membrane, as well as a rapid increase in TSPO ligand binding. [16, 32]

Amino acids deletion, site-directed mutagenesis and structural studies have permitted to identified a *cholesterol recognition amino acid consensus* (*CRAC*) sequence in the cytosolic carboxy-terminal domain of the TSPO that could be part of the binding site for the uptake and translocation of cholesterol (*channel-like interaction*) through a channel delimited by five α-helixes of TSPO. Besides, for cholesterol delivery into mitochondria TSPO-mediated is also required the interaction of TSPO with StAR, as referred above, a protein acting as hormoneinduced activator. [6, 16, 32]

It has been observed a relationship between steroid levels, TSPO levels and anxiety, principally due to the fact that neurosteroids are endogenous modulators of the $GABA_A$ receptor (**Figure 7**).

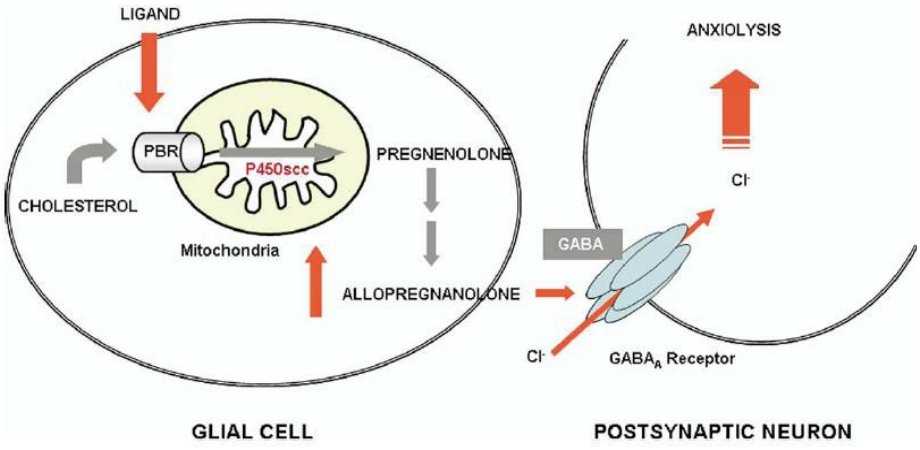


**Figura 7.** Schematic representation of TSPO-mediated regulation of neurosteroid biosynthesis and its role in neurological disorders.[19]

TSPO levels, determined by radioligand binding to platelets, decrease in patients with anxiety disorders. Therefore, ligands binding to TSPO located in glial cells, as well as *N,N*-dialchyl-2-pheniylindol-3-ylglyoxylamides synthesized by Da Settimo et al.[34], provide the cholesterol necessary to restore neurosteroid synthesis and increase pregnenolone formation, which is then metabolize to form allopregnanolone, a potent allosteric modulator of the $GABA_A$ exerting anxiolytic effects. For this reason, TSPO could be considering a promising target for the psychiatric disorders that involve dysfunction in steroid biosynthesis.[19, 35]

- **Other Functions:** TSPO has got other functions, for example: *protein import*, important for membrane biogenesis and in fact TSPO is necessary for the import of StAR protein into mitochondria; *TSPO binding of dicarboxylic porphyrin and transport* into mitochondria and in particular the relationship between TSPO and *heme biosynthesis* pathway; *ion transport* and *calcium homeostasis* (TSPO regulates the $Ca^{2+}$ flow into the cell); TSPO has got an important role in *cellular respiration, mitochondrial oxidation*, *cellular proliferation and differentiation* in a number of cell types.[6] TSPO can modulate responses to viral infections. In fact, pathogenic virus targets TSPO to inhibit dissipation of the transmembrane mitochondrial potential and prevents the release of *cytochrome c*, resulting in the blockade of apoptosis and overcoming of the host responses against viral infections.[28]

# TSPO Ligands

TSPO has got two different types of ligands: **endogenus** and **synthetic**.

- **Endogenus Ligands:** a numerous types of endogenous molecules with affinity for the TSPO and different chemical structures have been identified.

*Protoporphyrins* (protoporphyrins IX, mesoporphyrins IX, deuteroporphyrins IX, hemin) have got a high affinity for TSPO. As several steroidogenic tissues, as well as the adrenal gland and testis, show high TSPO and porphyrin levels, it has been suggested a physiological role for the interaction of these two molecules. Furthermore, having a plane of symmetry (**Figure 8**), these molecules could bind dimerized form of TSPO, confirming in this way the postulated two-binding site model. [16, 33]

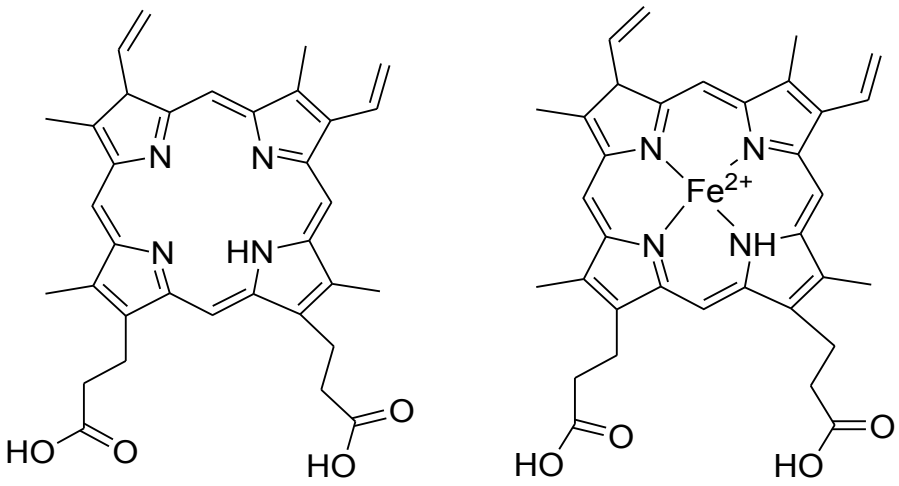


**(3)** **(4)**

**Figure 8**. Chemical structures of protoporphyrin IX (**3**) and heme (**4**).

*Cholesterol* is a important ligand as previously reported discussing the fundamental role of TSPO in the regulation of cholesterol transport and thus in the steroidogenesis. Again it has been shown that a dimeric form of TSPO possesses an enhanced binding capacity to cholesterol.[33]

In 1984 Corda et al. isolated and purified a neuropeptide able to inhibit diazepam binding to BZ binding site on brain membranes. This 11 kDa polypeptide, named *DBI (diazepam binding inhibitor),* is constituted by 86 amino acids and binds with low affinity both TSPO and CBR, while a short fragment of DBI, triakontatetra-neuropeptide, is more selective for TSPO. Furthermore, DBI promotes loading of cholesterol to the cytochrome P450scc and

stimulates steroidogenesis by directly interacting with TSPO.[32, 33]
*Anthralin* is a 16 kDa protein that has been demonstrated interact with both TSPO and dihydropyridine binding site, and *phospholipase A2* have also been proposed as endogenous ligands for TSPO.[33]

- **Synthetic Ligands:** this ligands have been developed with the aim to deepen the knowledge of the exact pharmacological role of TSPO, to define its involvement in several pathophysiological conditions and to establish the structural requirements needed for an optimum of affinity.
  Initially, the most of these ligands have been designed starting from classical selective CBR ligands, as well as benzodiazepines, making the necessary structural modifies in order to shift the affinity toward TSPO. Until to date the prototypic ligands, used as reference compounds in the development of TSPO pharmacophore models and in *SAR* (*structure-activity relationship*) studies, are the benzodiazepine Ro 5-4864 **(2)** and the isoquinolinecarboxamide PK11195 **(5)**, classified by LeFur and coworkers the first as a TSPO agonist or partial agonist and the second as an antagonist.[16]
  Then, a number of diversified structures have been developed with good results of affinity and selectivity, and leading to drawing various TSPO pharmacophore models useful for designing novel synthetic derivatives. Therefore, the topology of the TSPO binding cleft has not yet been completely defined.[5]

  TSPO specific synthetic ligands do not have a typical shared structure and thus can be distinguished nine different classes of compounds (**Figure 9**).

1) **Benzodiazepines:** in this class the selectivity toward the TSPO or CBR results very sensitive even to slight structural modifications: in fact, as described earlier in **Figure 1**, in the case of Ro 5-4864 **(2)** the insertion of a chlorine at the para position of the pendant phenyl rings of the diazepam, equipotent at the two receptors, shifts the selectivity toward TSPO. Ro 5-4864 has been used in a number of studies aimed at characterizing TSPO, and particularly by Gavioli and colleagues to study the putative role of TSPO as a target for the treatment of psychiatric disorders.[5]

2) **Isoquinolinecarboxamide** PK 11195 **(5)** is the first non-benzothiazepine ligand binding the TSPO with nanomolar affinity and it is widely used for studies aimed to define and map the binding site. In 2008, Chelli et al.[36] showed that treatment of a human astrocytoma cell line (ADF) with PK 11195 actives an autophagic pathway followed by apoptosis mediated by mitochondrial potential dissipation. Moreover, has been showed that PK 11195 has a multidrug resistance modulating activity increasing the efficacy of a daunorubicin treatment on human multidrug-resistant leukemia cell line in vitro by 5-7 fold and blocking p-glycoprotein efflux, a transporter whose activity contributes to limit antitumor drug efficacy.[28]

3) Alpidem **(6)** can be considered the progenitor of the class of **imidazopyridines**

known to bind both TSPO and CBR with the nanomolar affinity (K*i* 0.5-7 nM and 1-28 nM, respectively).[5]

4) **Phenoxyphenylacetamide** derivatives, such as DAA1097 **(7)**, were designed by a process of molecular simplification involving the opening of the diazepine ring of Ro 5-4864. Some compounds of this class of TSPO ligands have also showed potent anxiolytic properties in laboratory animals.[5]

5) **Pyrazolopyrimidineacetamides**, i.e. DPA714 **(8)**, were first described by Selleri and coworkers as bioisosters of the imidazopyridines and thereby closely related to alpidem.[5]

6) **Indoleacetamide** derivatives, collectively named FGIN-1 **(9)**, was developed by Kozikowski and colleagues as a new class of compounds binding with high affinity and selectivity for TSPO. [5] In a recent study SSR180575 **(10)**, an indoleacetamide compound, was shown to have neuroprotective properties in different models of progressive degeneration of the PNS and CNS: precisely it promotes neuronal survival and repair following axotomy through the regulation of apoptosis of glial cells and/or the production of mediators such as neurosteroids, cytokines or other neurotrophic factors that support nerve survival.[28]

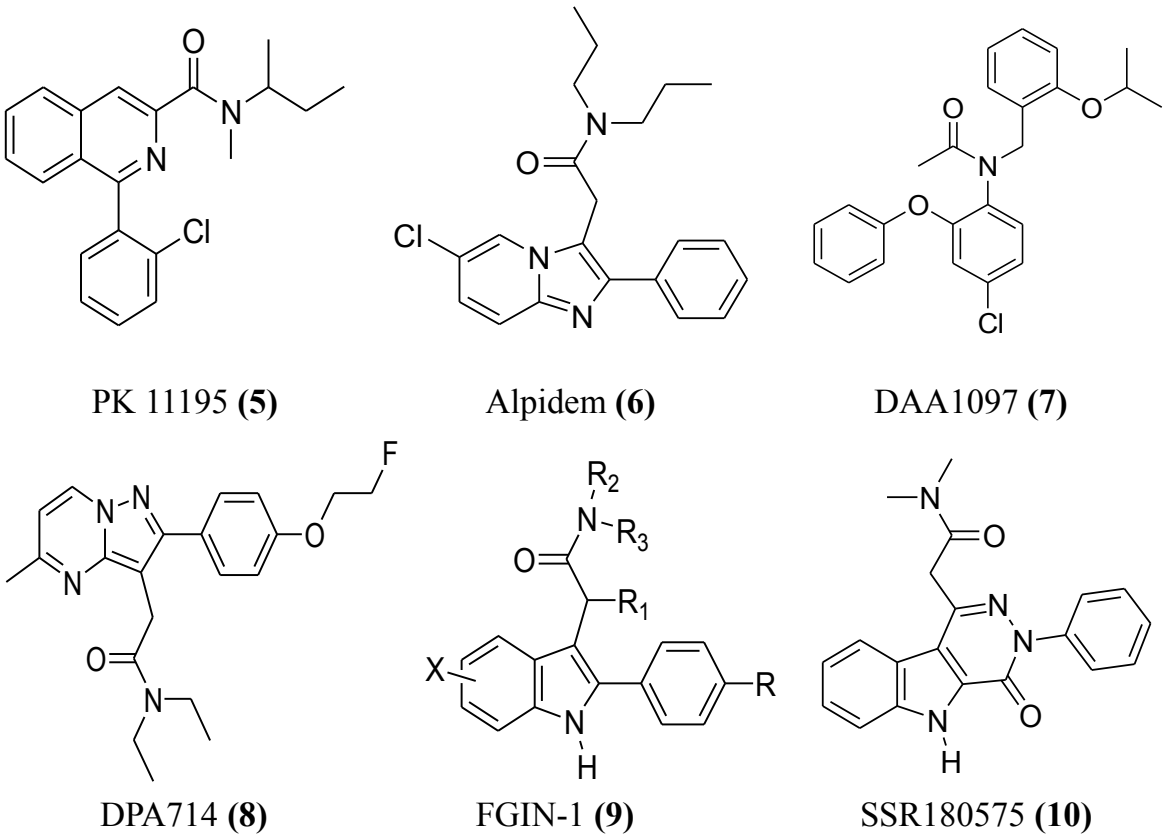


**Figure 9.** Structures of the some representative ligands of the most important classes of compounds selective for TSPO.

7) **Benzothiazepines**, a class of TSPO ligands featuring a 6,7 bicyclic nucleus, were initially developed by Campiani and coworkers as selective ligands for CBR and GABA receptor subtypes. Some pyrrolobenzothiazepines derivatives possess an unexpected significant inhibitory activity at L-type calcium channels, equal to or higher than those of reference calcium antagonists such as verapamil and (+)-*cis*-diltiazem.[5]

8) On the basis of pyrrolobenzothiazepine skeleton, the **pyrrolobenzoxazepine** scaffold has been developed, featuring the replacement of the endocyclic sulfur ($S_5$) with an oxygen ($O_5$), that increases affinity by 2-3 fold. Some of these compounds showed an high affinity toward the TSPO (K*i* values in the low nanomolar-subnanomolar range) and the capacity to stimulate steroidogenesis in mouse Y-1 adrenocortical cell line.[5]

9) **Indol-3-ylglyoxylamides** (this class is treatise in the next section).

# N,N-Dialkyl-2-phenylindol-3-ylglyoxylamides

In 2004 Primofiore et al.[37] prepared and tested a series of *N,N*-dialkyl-2-phenylindol-3-ylglyoxylamide derivatives **I** (**Table 1**) as TSPO ligands, designed as conformationally constrained analogues of the indoleacetamides of the FGIN (**9**) series previously described by Kozikowski and coworkers. Most of these compounds showed a high affinity for TSPO in the nanomolar to subnanomolar range and a high selectivity for TSPO over CBR. The TSPO/CBR selectivity was evaluated by binding studies using membranes from rat brain tissues and [$^3$H]flumazenil as radioligand. For some of these TSPO ligands with high affinity, the ability to stimulate pregnenolone formation from rat C6 glioma cells was evaluated.

In **Table 1** has been reported the binding affinity of compounds **Ia-Iaah** (data taken from ref. 34, 37) and of the standard TSPO ligands Ro 5-4864 (**2**), PK 11195 (**5**) and alpidem (**6**), expressed as K*i* values.

It has been observed that, among the unsubstitued derivatives **Ia-Im (**$R_3 = R_4 = R_5 = R_6 =$ H**)**, N-monosubstitued compounds **Ia-Ib** show the lowest affinity probably because they cannot occupy both the L3 and L4 lipophilic pockets.
The *N,N*-disubstitued indolylglyoxylamides instead exhibit a high affinity and in particular compound **Ig,** bearing two *n*-hexyl groups, is the most potent, with a K*i* of 1,4 nM. Therefore, increasing the length of the linear N-alkyl groups has been observed an enhancement of affinity, due to the better filling of L3 and L4 lipophilic pockets. [37]

The three derivatives **Id**, **Ie**, **Ig** and **Ij** has been selected as leads for further affinity optimization efforts. It has been observed that: [5, 34, 37]

- The insertion of an electron-donating lipophilic group, as well as a methyl group (**Idd-Igg**), in the 4'-position ($R_3$) of the 2-phenyl ring does not produce any gain in affinity respect to the parent unsubstitued compound. Introducing an electron- withdrawing substituent as well as Cl, F, $NO_2$ and $CF_3$ (**In-Icc**), it has been instead obtained compounds with higher affinity, and among these ones, the *N,N*-di- *n*-hexyl derivatives **Ip** (Cl), **It** (F), **Ix** ($NO_2$) and **Ibb** ($CF_3$) have been revealed the most potent, with K*i* values of o.37 nM, 0.55 nM, 0.27 nM and 1 nM, respectively. These results suggest that the $R_3$ substituent has to be electron-withdrawing to reinforce the putative π-stacking interaction with an electron-rich aromatic ring within the L1 pocket.

- The data of affinity of compounds **Ihh-Iww** bearing a substituent in the 5-position of the indole nucleus (F, Cl, $NO_2$, $OCH_3$) suggest that $R_6$ has to be electron-withdrawing and also very small for optimal binding, and only **Ijj** with a fluorine at the 5-position features these properties (K*i* = 0.37 nM).

- The introduction of two halogens in both 4'- and 5-positions (**Ixx-Iiii**;**Ivvv-Iyyy**) does not increase affinity in additive manner, but it has supposed a

correlation with the nature of the *N,N*-dialkyl chain.

- Substitutions at the 7-position of the indole nucleus ($R_5$) with an electron-withdrawing (Cl, **Ijjj-Immm**) or an electron-donating ($CH_3$, **Innn-Iqqq**) lipophilic group do not produce any gain in affinity.

- The binding data of asymmetrical *N,N*-dialkyl derivatives (**Irrr-Iaah**), designed to probe the L3 and L4 lipophilic pockets at the TSPO binding site, indicate that the L3 and L4 pockets are probably different in their dimensions, and that $R_1$ and $R_2$ have to be of different size to obtain the bestperforming substitution on the amide nitrogen. Therefore, an aromatic moiety on $R_1$/$R_2$ substituents is equivalent to an aliphatic moiety of similar size in interacting with the two lipophilic pockets.

**Table 1.** TSPO binding affinity of *N,N*-dialkylindolylglyoxylamide derivatives **Ia-Iaah**.

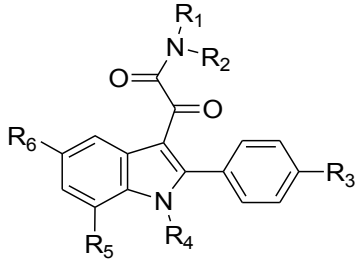

**I**

| n | $R_1$ | $R_2$ | $R_3$ | $R_4$ | $R_5$ | $R_6$ | Ki (nM) or inhinibition (%)[c] | |
|---|---|---|---|---|---|---|---|---|
| | | | | | | | TSPO[a] | CBR[b] |
| **Ro 5-4864** | | | | | | | 23.0 ±3.0 | |
| **PK 11195** | | | | | | | 9.30±0.5 | |
| **alpidem** | | | | | | | 0.5-7 | 1-28 |
| **Ia** | $(CH_2)_2CH_3$ | H | H | H | H | H | 815 ±80 | 3293±381 |
| **Ib** | $(CH_2)_3CH_3$ | H | H | H | H | H | 1167±99 | 12% |
| **Ic** | $CH_2CH_3$ | $CH_2CH_3$ | H | H | H | H | 43.0±4 | |
| **Id** | $(CH_2)_2CH_3$ | $(CH_2)_2CH_3$ | H | H | H | H | 12.2±1.0 | 16% |
| **Ie** | $(CH_2)_3CH_3$ | $(CH_2)_3CH_3$ | H | H | H | H | 7.5±0.7 | 3% |
| **If** | $(CH_2)_4CH_3$ | $(CH_2)_4CH_3$ | H | H | H | H | 16.0±2.0 | 3% |
| **Ig** | $(CH_2)_5CH_3$ | $(CH_2)_5CH_3$ | H | H | H | H | 1.4±0.2 | 10% |
| **Ih** | $CH(CH_3)_2$ | $CH(CH_3)_2$ | H | H | H | H | 103±9.0 | |
| **Ii** | $CH(CH_3)CH_2CH_3$ | $CH(CH_3)CH_2CH_3$ | H | H | H | H | 17.0±2.0 | 5% |
| **Ij** | $CH_2CH_3$ | $CH_2C_6H_5$ | H | H | H | H | 11.0±1.0 | |
| **Ik** | $-(CH_2)_4-$ | | H | H | H | H | 2400±125 | 4% |
| **Il** | $-(CH_2)_5-$ | | H | H | H | H | 665±30 | 3% |
| **Im** | $-(CH_2)_6-$ | | H | H | H | H | 33.0±3.0 | 3% |
| **In** | $(CH_2)_2CH_3$ | $(CH_2)_2CH_3$ | F | H | H | H | 4.28±0.32 | 4.3% |
| **Io** | $(CH_2)_3CH_3$ | $(CH_2)_3CH_3$ | F | H | H | H | 2.40±0.81 | 0% |

| | | | | | | | | |
|---|---|---|---|---|---|---|---|---|
| **Ip** | $(CH_2)_5CH_3$ | $(CH_2)_5CH_3$ | F | H | H | H | 0.37±0.13 | 0% |
| **Iq** | $CH_2CH_3$ | $CH_2C_6H_5$ | F | H | H | H | 1.68±0.12 | 10% |
| **Ir** | $(CH_2)_2CH_3$ | $(CH_2)_2CH_3$ | Cl | H | H | H | 4.65±0.52 | 14% |
| **Is** | $(CH_2)_3CH_3$ | $(CH_2)_3CH_3$ | Cl | H | H | H | 1.00±0,27 | 0% |
| **It** | $(CH_2)_5CH_3$ | $(CH_2)_5CH_3$ | Cl | H | H | H | 0.55±0.19 | 4.2% |
| **Iu** | $CH_2CH_3$ | $CH_2C_6H_5$ | Cl | H | H | H | 1.30±0.15 | 7.3% |
| **Iv** | $(CH_2)_2CH_3$ | $(CH_2)_2CH_3$ | $NO_2$ | H | H | H | 0.95±0.1 | |
| **Iw** | $(CH_2)_3CH_3$ | $(CH_2)_3CH_3$ | $NO_2$ | H | H | H | 0.23±0.07 | |
| **Ix** | $(CH_2)_5CH_3$ | $(CH_2)_5CH_3$ | $NO_2$ | H | H | H | 0.27±0.10 | |
| **Iy** | $CH_2CH_3$ | $CH_2C_6H_5$ | $NO_2$ | H | H | H | 0.55±0.02 | |
| **Iz** | $(CH_2)_2CH_3$ | $(CH_2)_2CH_3$ | $CF_3$ | H | H | H | 1.69±0.2 | |
| **Iaa** | $(CH_2)_3CH_3$ | $(CH_2)_3CH_3$ | $CF_3$ | H | H | H | 1.16±0.1 | |
| **Ibb** | $(CH_2)_5CH_3$ | $(CH_2)_5CH_3$ | $CF_3$ | H | H | H | 1.0±0.1 | |
| **Icc** | $CH_2CH_3$ | $CH_2C_6H_5$ | $CF_3$ | H | H | H | 1.0±0.1 | |
| **Idd** | $(CH_2)_2CH_3$ | $(CH_2)_2CH_3$ | $CH_3$ | H | H | H | 5.50±0.98 | |
| **Iee** | $(CH_2)_3CH_3$ | $(CH_2)_3CH_3$ | $CH_3$ | H | H | H | 3.80±0.91 | |
| **Iff** | $(CH_2)_5CH_3$ | $(CH_2)_5CH_3$ | $CH_3$ | H | H | H | 1.60±0.13 | |
| **Igg** | $CH_2CH_3$ | $CH_2C_6H_5$ | $CH_3$ | H | H | H | 2.64±0.1 | |
| **Ihh** | $(CH_2)_2CH_3$ | $(CH_2)_2CH_3$ | H | H | H | F | 2.67±0.48 | |
| **Iii** | $(CH_2)_3CH_3$ | $(CH_2)_3CH_3$ | H | H | H | F | 4.00±0.15 | |
| **Ijj** | $(CH_2)_5CH_3$ | $(CH_2)_5CH_3$ | H | H | H | F | 0.37±0.12 | |
| **Ikk** | $CH_2CH_3$ | $CH_2C_6H_5$ | H | H | H | F | 1.33±0.2 | |
| **Ill** | $(CH_2)_2CH_3$ | $(CH_2)_2CH_3$ | H | H | H | Cl | 2.80±0.3 | 10% |
| **Imm** | $(CH_2)_3CH_3$ | $(CH_2)_3CH_3$ | H | H | H | Cl | 4.91±0.4 | 13% |
| **Inn** | $(CH_2)_5CH_3$ | $(CH_2)_5CH_3$ | H | H | H | Cl | 58.4±6 | 3% |
| **Ioo** | $CH_2CH_3$ | $CH_2C_6H_5$ | H | H | H | Cl | 4.6±0.5 | |

| | | | | | | | | |
|---|---|---|---|---|---|---|---|---|
| **Ipp** | $(CH_2)_2CH_3$ | $(CH_2)_2CH_3$ | H | H | H | $NO_2$ | 20.2±2.02 | 0% |
| **Iqq** | $(CH_2)_3CH_3$ | $(CH_2)_3CH_3$ | H | H | H | $NO_2$ | 21.6±2.15 | 1% |
| **Irr** | $(CH_2)_5CH_3$ | $(CH_2)_5CH_3$ | H | H | H | $NO_2$ | 30.3±9.15 | 0% |
| **Iss** | $CH_2CH_3$ | $CH_2C_6H_5$ | H | H | H | $NO_2$ | 18.3±0.15 | 0% |
| **Itt** | $(CH_2)_2CH_3$ | $(CH_2)_2CH_3$ | H | H | H | $OCH_3$ | 328±45 | 8.6% |
| **Iuu** | $(CH_2)_3CH_3$ | $(CH_2)_3CH_3$ | H | H | H | $OCH_3$ | 65.2±3.4 | 8.8% |
| **Ivv** | $(CH_2)_5CH_3$ | $(CH_2)_5CH_3$ | H | H | H | $OCH_3$ | 35.5±8.7 | 7.2% |
| **Iww** | $CH_2CH_3$ | $CH_2C_6H_5$ | H | H | H | $OCH_3$ | 69.5±3.6 | 5.7% |
| **Ixx** | $(CH_2)_2CH_3$ | $(CH_2)_2CH_3$ | F | H | H | Cl | 2.83±0.08 | 14% |
| **Iyy** | $(CH_2)_3CH_3$ | $(CH_2)_3CH_3$ | F | H | H | Cl | 3.05±0.45 | 17% |
| **Izz** | $(CH_2)_5CH_3$ | $(CH_2)_5CH_3$ | F | H | H | Cl | 7.75±1.55 | |
| **Iaaa** | $CH_2CH_3$ | $CH_2C_6H_5$ | F | H | H | Cl | 4.01±0.26 | 9.7% |
| **Ibbb** | $(CH_2)_2CH_3$ | $(CH_2)_2CH_3$ | F | H | H | F | 6.73±1.39 | |
| **Iccc** | $(CH_2)_3CH_3$ | $(CH_2)_3CH_3$ | F | H | H | F | 4.36±0.05 | |
| **Iddd** | $(CH_2)_5CH_3$ | $(CH_2)_5CH_3$ | F | H | H | F | 0.95±0.1 | |
| **Ieee** | $CH_2CH_3$ | $CH_2C_6H_5$ | F | H | H | F | 1.67±0.37 | |
| **Ifff** | $(CH_2)_2CH_3$ | $(CH_2)_2CH_3$ | Cl | H | H | Cl | 0.62±0.06 | 5% |
| **Iggg** | $(CH_2)_3CH_3$ | $(CH_2)_3CH_3$ | H | H | H | Cl | 1.9±0.2 | 0% |
| **Ihhh** | $(CH_2)_5CH_3$ | $(CH_2)_5CH_3$ | H | H | H | Cl | 5.8±0.6 | 3% |
| **Iiii** | $CH_2CH_3$ | $CH_2C_6H_5$ | H | H | Cl | Cl | 3.33±0.3 | |
| **Ijjj** | $(CH_2)_2CH_3$ | $(CH_2)_2CH_3$ | H | H | Cl | H | 14.0±1.5 | 0% |
| **Ikkk** | $(CH_2)_3CH_3$ | $(CH_2)_3CH_3$ | H | H | Cl | H | 3.40±0.3 | 1% |
| **Illl** | $(CH_2)_5CH_3$ | $(CH_2)_5CH_3$ | H | H | Cl | H | 2.4±0.3 | 0% |
| **Immm** | $CH_2CH_3$ | $CH_2C_6H_5$ | H | H | $CH_3$ | H | 5.0±0.4 | 0% |
| **Innn** | $(CH_2)_2CH_3$ | $(CH_2)_2CH_3$ | H | H | $CH_3$ | H | 25.0±3.0 | |
| **Iooo** | $(CH_2)_3CH_3$ | $(CH_2)_3CH_3$ | H | H | $CH_3$ | H | 6.0±0.6 | |
| **Ippp** | $(CH_2)_5CH_3$ | $(CH_2)_5CH_3$ | H | H | $CH_3$ | H | 1.90±0.1 | |

| | | | | | | | | |
|---|---|---|---|---|---|---|---|---|
| Iqqq | $CH_2CH_3$ | $CH_2C_6H_5$ | H | H | $CH_3$ | H | 2.30±0.2 | |
| Irrr | $CH_3$ | $CH_2CH_3$ | H | H | H | H | 940±120 | 15% |
| Isss | $CH_3$ | $(CH_2)_3CH_3$ | H | H | H | H | 53.3±4.0 | |
| Ittt | $CH_3$ | $(CH_2)_4CH_3$ | H | H | H | H | 12.1±1.0 | |
| Iuuu | $CH_2CH_3$ | $(CH_2)_3CH_3$ | H | H | H | H | 12.6±1.0 | |
| Ivvv | $CH_3$ | $CH_2CH_3$ | Cl | H | H | Cl | 9.54±1.29 | 15% |
| Iwww | $CH_3$ | $(CH_2)_3CH_3$ | Cl | H | H | Cl | 0.15±0.02 | |
| Ixxx | $CH_3$ | $(CH_2)_4CH_3$ | Cl | H | H | Cl | 0.18±0.02 | |
| Iyyy | $CH_2CH_3$ | $(CH_2)_3CH_3$ | Cl | H | H | Cl | 0.36±0.04 | |
| Izzz | $CH_3$ | $CH_2C_6H_5$ | H | H | H | H | 12.0±1.0 | |
| Iaab | $CH_3$ | $CH_2C_6H_5$ | F | H | H | H | 1.8±0.1 | |
| Iaac | $CH_3$ | $(CH_2)_3CH_3$ | Cl | H | H | H | 11±1.0 | |
| Iaad | $CH_3$ | $(CH_2)_4CH_3$ | Cl | H | H | H | 3.4±0.4 | |
| Iaae | $CH_2CH_3$ | $(CH_2)_3CH_3$ | Cl | H | H | H | 3.6±0.4 | |
| Iaaf | $CH_3$ | $(CH_2)_3CH_3$ | H | H | H | Cl | 3.9±0.5 | |
| Iaag | $CH_3$ | $(CH_2)_4CH_3$ | H | H | H | Cl | 3.6±0.5 | |
| Iaah | $CH_2CH_3$ | $(CH_2)_3CH_3$ | H | H | H | Cl | 1.8±0.2 | |

[a] The concentration of tested compounds that inhibited [$^3$H]PK 11195 binding to rat kidney mitochondrial membranes ($IC_{50}$) by 50% was determined with six concentrations of the displacers, each performed in triplicate. K*i* values are the mean ± SEM of three determinations. [b]The inhibition percent of [$^3$H]flumazenil specific binding at 10 μM of the compound are the mean ± SEM of five determinations. K*i* values are the mean ± SEM of three determinations. [c] Data take from ref. 34, 37.

In 2008 Da Settimo et al. [34] refined TSPO pharmacophore/topological model through the synthesis and the biological evaluation of novel indole derivatives with the general formula **I**, bearing different combinations of substituents $R_1$-$R_6$.

The SARs of these compounds were rationalized in light of a pharmacophore/topological model of TSPO binding site made up of three lipophilic pockets (L1, L3 and L4) and a H-bond donor group (H1) (**Figure 10**). Specifically:

1. the second carbonyl group of the oxalyl bridge engages an H-bond with the donor site H1;
2. the two lipophilic substituents $R_1$ and $R_2$ (linear or ramified alkyl, arylalkyl group) on the amide nitrogen interact hydrophobically with the L3 or L4 lipophilic pockets;
3. the 2-phenyl group establishes π-stacking interactions within the L1 pocket.

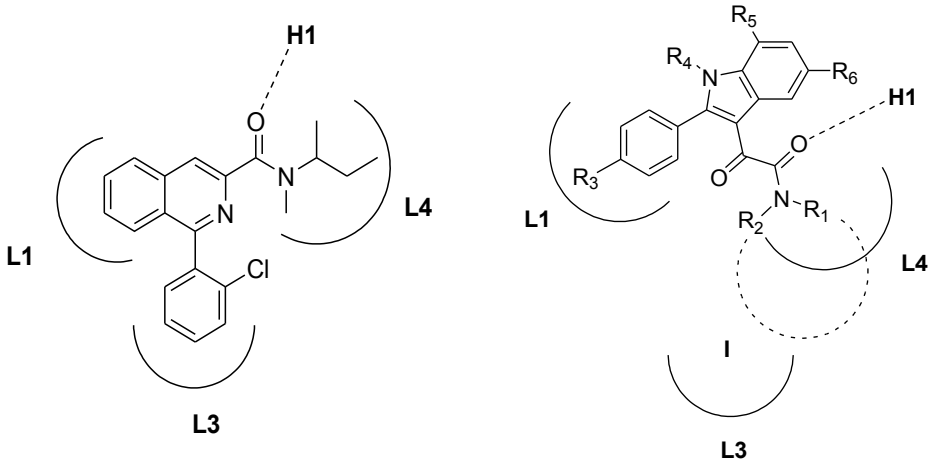


PK 11195 N,N-dialkyl-2-phenylindol-3-ylglyoxylamies (**I**)

**Figure 10.** TSPO pharmacophore/topological model.

# Molecular probes

Diagnostic imaging is referred to different imaging modalities and technologies, as well as:

- Radiography;
- Nuclear Imaging:
  - PET (Positron Emission Tomography);
  - SPECT (Single Photon Emission Computed Tomography);
  - PET/CT (PET/Computed Tomography combination).
- Magnetic Resonance Imaging (MRI);
- Optical Imaging
  - fluorescence;
  - near-infrared or NIR.
- Diagnostic Ultrasounds.

Some of these imaging methods are based on use of molecular probes and for this reason can be called "molecular imaging" modalities. Molecular probes can be referred to radiolabelled molecules or fluorescent ligands designed for in vitro or in vivo application, able to form covalent bindings with apposite constituents of receptor (affinity labels) and therefore useful for determination and characterization of a receptor by various chemical-physical techniques.
Molecular probes consist of two parts: [35]

1. a radioactive nuclide or a fluorophore group, responsible for a signal detectable outside of the organism for visualization with nuclear medical methods or fluorescent spectroscopy;

2. a molecular structure (vector, ligand, vehicle), that defines the biological characteristics and is responsible for chemical and biochemical interactions within the living organism, influencing in this way pharmacokinetic and pharmacodynamic parameters.

   Since they are chemically indistinguishable from their non-radioactive counter-parts, molecular probes either interact directly with specific target sites and processes (substrates for enzymes, ligands for receptors or transporters) or take part directly in metabolic processes. For these reasons they can be used for in vitro or in vivo visualization, characterization and quantification of biological processes at the cellular and subcellular level.[38]

Molecular imaging is also a non-invasive biomedical instrument useful for the diagnosis and monitoring of cardiac pathology, different forms of cancer and neurological diseases. Imaging methods also allows monitoring the progression of a pathology in a specific patient, permitting an approach of personalized therapy and visualizing a pathological change on the molecular level resulting in abnormal function long before morphological manifestation.[38]

# Molecular probes used for TSPO

The density of TSPO is much increased in several human pathologies, such as gliomas and neurodegenerative disorders, for example Huntington's and Alzheimer's diseases, as well as in various forms of brain injury and inflammation. TSPO is also up-regulated in neuroinflammatory conditions mediated by microglial activation. Changes in TSPO levels have also been detected in patients affect by generalized anxiety, panic, post-traumatic stress, obsessive-compulsive disorders, and separation anxiety. [39]
For this reasons, TSPO has been suggested as a promising diagnostic marker to image and measure the TSPO expression and distribution levels in living cells, isolated tissues, or living subjects, and then for evaluation of disease progression by mean of specific fluorescent or radiolabeled ligands.
PET imaging using TSPO ligands to label activated microglia offers quantitative measures of inflammation and then can help to understand the regional brain distribution, stage and severity of neuroinflammation, so can be considered a valuable tool to determine individual approaches to treatment of disease. [39]
Fluorescent ligands is a alternative to radioligands for investigating the localization and the expression level of TSPO. In 2010 Taliani and coworkers[41] developed novel potent, selective and irreversible fluorescent probes introducing a NBD-fluorophore (7-nitrobenz-2-oxa-1,3-diazol-4-yl) and an electrophilic isothiocyanato group on the 2-phenylindolylglyoxylamide scaffold.

# Imaging using PET

PET (Positron Emission Tomography) is one of the most important imaging technique in the field of nuclear medicine, able to detect nanomolar metabolic variations. Originally used primarily as a research tool, PET has also had an increasingly important clinical role. There are four major areas of clinical application: oncology (diagnosis and monitoring of tumor, follow up therapy, tumor prognosis evaluation), cardiology (metabolism and myocardial viability), neurology (epilepsy, schizophrenia, Parkinson, Alzheimer) and psychology ("sensorial emotional images"). [38]
PET is a radiotracer imaging technique which uses small amounts of tracer compound labeled with positron-emitting radionuclides (called radiopharmaceutical or radiotracer) to help in the diagnosis of disease. Therefore, in PET short-lived radioactive drug emitting gamma rays is introduced in the subject of the study, either by injection or inhalation of a gas, and after an appropriate uptake period its concentration in tissue is measured by a PET scanner, which produce an image showing its distribution in the body. [41] PET looks at

physiological processes rather than anatomical structures and then gives only functional information. Therefore, it may be difficult to accurately localized anatomic structures or lesions that exhibit abnormal radiotracer accumulation. This limitation can be overcome using PET/CT combination, which integrates the functional tissue information, that is provided by PET exam with the anatomical information, that can be obtained by structural imaging methods such as computed tomography (CT) exam, into one single exam. [42]

# The physical bases of PET

All the positron emitters have proton-rich nuclei, and, in an attempt to stabilized themselves by getting rid of the excess protons and gaining neutrons in lieu, they may decay via positron emission or electron capture, both of which are isobaric decay processes.[44]

In **Table 2** are showed some isotopes which decay via positron emission.

| Isotope | half-life (min) | Maximum positron energy (MeV) | Production method |
|---|---|---|---|
| **$^{11}$C** | 20.3 | 0.96 | cyclotron |
| **$^{13}$N** | 9.97 | 1.19 | cyclotron |
| **$^{15}$O** | 2.03 | 1.70 | cyclotron |
| **$^{18}$F** | 109.8 | 0.64 | cyclotron |
| **$^{68}$Ga** | 67.8 | 1.89 | generator |
| **$^{82}$Rb** | 1.26 | 3.15 | generator |

The positron is an antimatter electron, having the same mass but a positive charge. Schematically, the positron decay process can be represented by:

$$_{z}X \rightarrow {}_{z-1}X^{*} + e^{+} + \upsilon$$

There occurs a transmutation of elements: the daughter isotope has the same mass number but an atomic number reduced by one than the parent. This is accompanied by the emission of a neutrino, a particle with no mass or charge, and an highly interactive positron (small mass and positive charge). While the neutrino escapes without interacting in the surrounding material, the positron after travelling a short distance (3-5 mm) is showed down by the scattering processes in the electron clouds of the surrounding environment. The distance traveled by the positron is known as its range and is function of the PET isotopes and then of the positron energy ($^{18}$F, $^{11}$C, $^{15}$O, and $^{82}$Rb in water or tissue have a range between 2.6 and 16.5 mm). [42]
As positrons travel through human tissues, there is a continuous loss in kinetic energy

principally due to Coulomb interactions with electrons. When a positron reaches thermal energies, it combines with an electron either by annihilation, which produces two photons of 511 KeV each, or by the formation of a very short-lived particle called positronium (**Figure 11**).

$$e^+ + e^- \rightarrow \gamma + \gamma$$

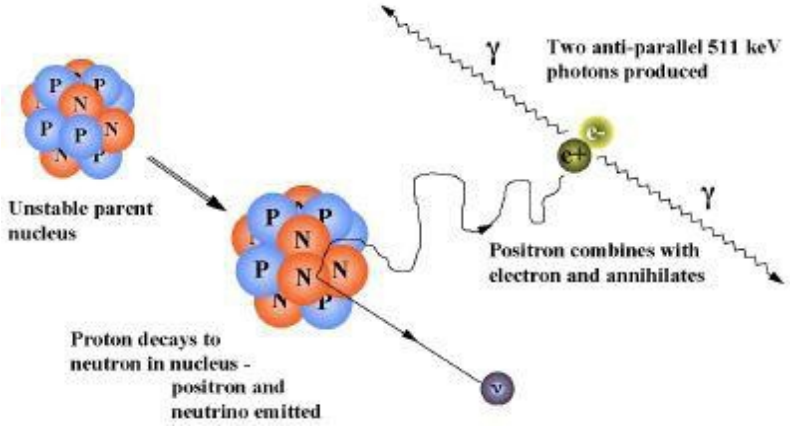


**Figure 11.** Positron emission and annihilation. [41]

The positronium is unstable and susceptible to the pick-off process, where it annihilates with another electron. In both cases the emitted pair of photons have an energy equivalent to the combined rest mass of an electron and a positron, and they are emitted at about 180° from each other.

The image acquisition is based on the detection of emitted γ-rays by the detectors surrounding the subject, which register the arrival of the annihilation photons as an event if the two detections occur within a narrow timing window (typically 3-15 ns). This "coincidence detection", termed electronic collimation, is a fundamental requirement of detection because is assumed that the annihilation of the same electronpositron couple takes place somewhere on the straight line drawn between the two detectors, termed line of response (LOR) or coincidence line.

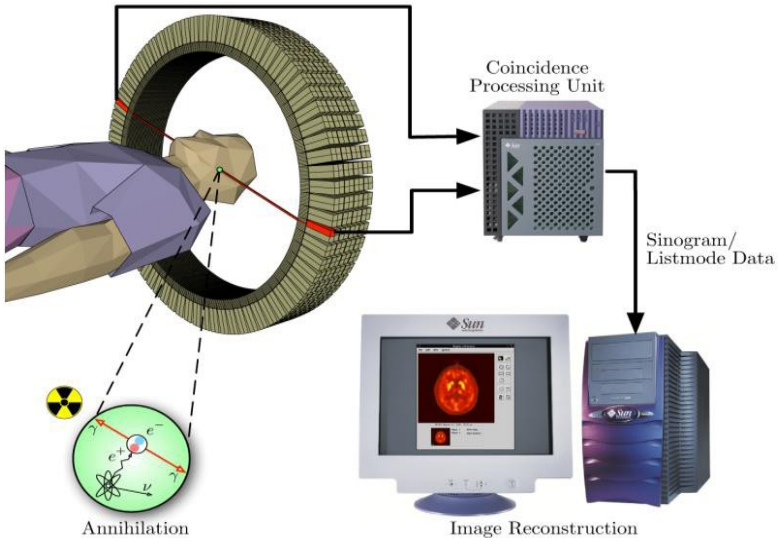


**Figure 12.** Coincidence detection (author Jens Langner).

These coincidence events provide information about the quantity and location of positrons: they are recorded and used in the image reconstruction through standard topographic techniques (**Figure 12**).[42]

## Factors limiting the spatial resolution of PET[42]

1. **Detector size.** The intrinsic detector spatial resolution also influences the quality of the reconstructed image. In modern PET scanners, the detectors use small crystal arrays coupled to large photodetectors.

2. **Non-colinearity of the annihilation photons.** Owing to some residual momentum of the positron before it combines with the electron, the annihilation photons are emitted at not exactly 180° from each other, resulting in a coincidence line usually shifted of a angle smaller than 0.5° leading to blurring in the image.

3. **Positron range.** PET scanner does not provide information on the distribution of positron emission points, because it detects γ-rays emitted at the annihilation point. Positron emission point and annihilation point generally are not coincident because, as referred earlier, positrons travel some distance (range) within the surrounding material before it combines with an electron and emits the annihilation photons.

# Pet radionucleotides

The choice of the radionuclide to be used in a PET exam is influenced by different considerations: [38]

- availability of the radionuclide;
- physical characteristics;
- radiochemical issues;
- radiopharmacological issues.

As reported earlier in **Table 2**, all widely used PET nuclides have a very short half-life with limited availability: this on the one hand ensures a low dose released to the patient, but on the other side limits the clinical applicability on a routine basis. Therefore the production of PET nuclides has to be performed in a medical cyclotron on-site. Only fluorine-18 and gallium-68 do not require a cyclotron in PET sites. [38] PET radionuclides are generally obtained from the cyclotron (or generator) in a chemical form that is not predisposed for direct labeling reactions and thus are required several primary activation steps. Activated radionuclides are subsequently incorporated into the chemical structure of the vehicle molecule.[38] A fundamental parameter that influences the imaging output is the specific radioactivity of the PET tracer, because a low specific activity would lead to low or undetectable signals: in the other words, the lower the density of the target sites the higher the required specific activity. [42]

# TSPO radioligands

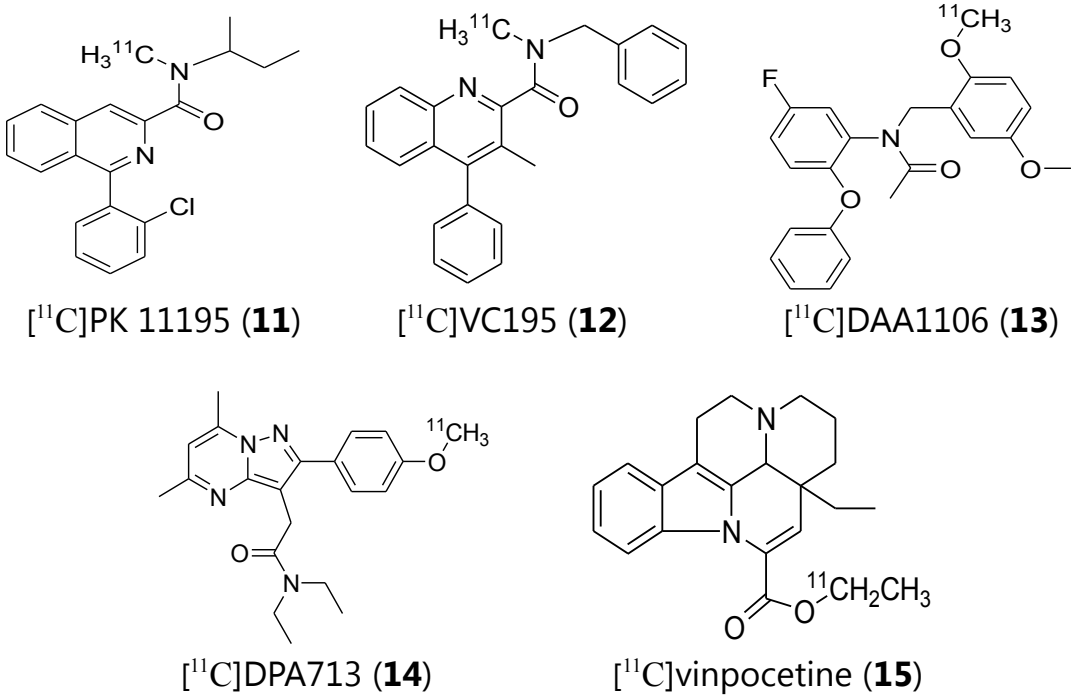


**Figure 13.** Chemical structures of various PET tracers for imaging of the TSPO.

1-(2-chlorophenyl-N-methyl-N-(1-methylpropil)-3-isoquinolinecarboxamide (PK11195, **5**) labeled with the positron emitter carbon-11 ($t_{1/2}$ = 20.4 min., $\beta^+$ = 99.8%) was the first TSPO radioligand to be used, first as racemate and later as R-enantiomer, in PET imaging of neurodegenerative pathologies, multiple sclerosis, brain tumors, cerebral infarct, and calcium channel anomalies in heart diseases. However, this radioligand presents several limitations, especially for brain imaging, including a high plasma protein binding and a poor penetration of the blood-brain barrier, which results in low levels of tracer in the brain. In addition, the high lipophilicity (log*P* = 3.4) of [$^{11}$C]PK 11195 (**11**) causes a high level of nonspecific binding and a poor signal-to-noise ratios that complicate its quantification and reduce its sensitivity in the in vivo evaluation of TSPO. Nevertheless, [$^{11}$C]PK 11195 (**11**) is still used as reference radioligand for the in vivo assessment of TSPO in PET studies.[39, 43] Subsequently, Matarrese et al.[44] labeled new conformationally restrained quinoline-2-carboxamide derivatives analogues of PK 11195 (**5**) as potential radioligands to investigate TSPO in vivo. The radioligands were synthesized by [$^{11}$C]-N-methylation from the corresponding desmethyl precursors. Among the compounds assayed, radioligand N-[$^{11}$C]-VC195 (**12**), demonstrating a highly specific binding and tissue-to-blood ratios, emerged of potential interest for in vivo PET monitoring of neurodegenerative processes, but at the same time the high background levels of the tracer in the brain reduce its sensitivity.[43] Even several phenoxyphenylacetamide derivatives, such as [$^{11}$C]DAA1106 (**13**), were radiolabeled with carbon-11 for PET imaging of TSPO. Zhang and co-workers [45] observed that these radioligands pass across the blood-brain barrier, enter the rat brain and preferably distribute in the olfactory bulb and cerebellum, where there is the richest TSPO density in the rat brain. The binding specificity to the TSPO in the rat brain was demonstrated through the co-injection of non-radiolabeled TSPO-selective ligands resulting in a strong reduction of tracer up-take in the both brain regions. [$^{11}$C]DAA1106 (**13**) has been reported to be able to detect activation of microglia in several rat models of inflammations.

☯C]DPA713 (**14**) is a pyrazolopyrimidine derivative proposed as a PET tracer for the TSPO because has a lower lipophilicity, and higher selectivity and affinity (K*i* = 4.7 nM) toward the TSPO than [$^{11}$C]PK 11195 (K*i* = 9.3 nM). This TSPO antagonist was evaluated in vivo in a healthy baboon and it was observed a high-er signal-to-noise ratios than [$^{11}$C]-(*R*)-PK 11195 in a rat model of neurodegeneration, which makes [$^{11}$C]DPA713 suitable for quantification and studying of changes in the density of TSPO binding sites.[46]

Another example of TSPO radioligand is [$^{11}$C]vinpocetine (**15**), a Vinca minor alkaloid, that binds specifically the TSPO and used as a neuroprotective drug in the treatment and prevention of cerebrovascular diseases. [$^{11}$C]vinpocetine has showed a cerebral uptake 5-fold higher than that of [$^{11}$C]PK 11195 and a an he-terogeneous distribution in the brain of monkeys. It is mainly metabolized in [$^{11}$C]ethanol, that is showed not significantly contribute to the brain radioactivity pattern of [$^{11}$C]vinpocetine.[43]

# $N^1$-Methyl-2-Phenylindol-3-Ylglyoxylamides

*N,N*-dialkyl-(2-phenylindol-3-yl)glyoxylamides have been described as new potent and selective TSPO ligands, and then suitable for the development of novel PET radioligands for TSPO. SAR data and previously reported pharmacophore/topological model hypothesis (**Figure 14**) suggest that indole NH should not be involved in the recognition of the receptor protein. [39]

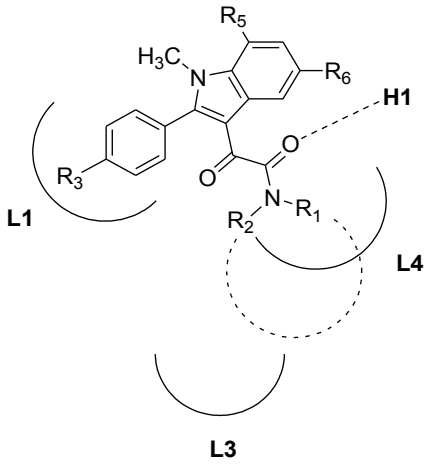


$N^1$-methyl-2-phenylindol-3-ylglyoxylamides

**Figure 14.** TSPO pharmacophore/topological model.

In 2011 Pike et al. [39] reported a novel series of 2-phenylindol-3-ylglyoxylamides featuring a methyl substituent on the indole nitrogen and showing a high affinity for TSPO, with K*i* values comparable to those of $N^1$-unsubstitued parent compounds. The binding data of $N^1$-methylated indoles **16-26**, expressed as K*i* values and determined in rat kidney membranes by binding competition experiments against [$^{11}$C]PK 11195 as radioligand, are listed in **Table 3**, and compared with those of the $N^1$-unbsustitued parent compounds (**Id**, **Ie**, **Ig**, **Ih**, **Ij**, **In**, **Ip**, **Iv**, **Isss**, **Ittt**, **Iuuu**, **Izzz**, **Iaab**) and the standard TSPO ligands **2**, **5**, and **6**.
All these compounds show K*i* values in the low nanomolar or subnanomolar range, from 0.3 to 0.60 nM, essentially comparable with those of their unsubstitued counterparts, and these data validate the hypothesis that the insertion of the methyl group at the $N^1$ position does not significantly influence TSPO binding. The compound **24** is the only exception, with the lowest K*i* value (K*i* = 190 nM), while compounds **17** and **18** possess the highest affinity in the series (K*i* = 0.30 nM) with a gain in activity of 25 and 4.6 fold respect to the unmethylated coun-terparts, **Ie** and **Ig**, respectively. [39]
The high affinity of the compounds **16-26** made them suitable for the development of radioligands for imaging brain TSPO with PET. The best candidate to be labeled at the $N^1$ position with the positron emitter carbon-11, by treatment with [$^{11}$C]methyl iodide and solid KOH in DMSO, is the compound **23** which shows the best combination of affinity (K*i* =5.7 nM), adequately high toward TSPO, and lipophilicity (cLog*P* =3.95), with a low nonspecific binding and a lipophilic/hydrophilic balance suitably moderate for crossing the

blood-brain barrier and achieving an adequate brain concentration. [39]

[$^{11}$C]**23** was synthesized by Pike and coworkers and tested with PET in rhesus monkeys, revealing a high proportion of radioligand to brain TSPO in the baseline experiments and furthermore the reversibility of this binding. Moreover, this radioligand was studied for the characteristics of its binding to brain membranes collected from a cohort of human subjects.

In conclusion, this research group has discovered a promising new chemotype for development of novel TSPO radioligands as biomarkers of neuroinflammation.

**Table 3.** TSPO binding affinity of *N,N*-dialkylindolylglyoxylamide derivatives **16-26** compared to those of the unmethylated counterparts (**Id**, **Ie**, **Ig**, **Ih**, **Ij**, **In**, **Ip**, **Iv**, **Isss**, **Ittt**, **Iuuu**, **Izzz**, **Iaab**).

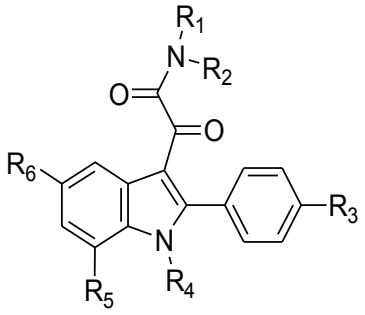


**I**

| n | $R_1$ | $R_2$ | $R_3$ | $R_4$ | $R_5$ | $R_6$ | Ki (nM) or inhinibition (%)[c] | |
|---|---|---|---|---|---|---|---|---|
| | | | | | | | TSPO[a] | CBR[b] |
| **Ro 5-4864** | | | | | | | 23.0 ±3.0 | |
| **PK 11195** | | | | | | | 9.30±0.5 | |
| **alpidem** | | | | | | | 0.5-7 | 1-28 |
| **Id** | $(CH_2)_2CH_3$ | $(CH_2)_2CH_3$ | H | H | H | H | 12.2±1.0 | 16% |
| **16** | $(CH_2)_2CH_3$ | $(CH_2)_2CH_3$ | H | $CH_3$ | H | H | 19.5±1.5 | |
| **Ie** | $(CH_2)_3CH_3$ | $(CH_2)_3CH_3$ | H | H | H | H | 7.5±0.7 | 3% |
| **17** | $(CH_2)_3CH_3$ | $(CH_2)_3CH_3$ | H | $CH_3$ | H | H | 0.300±0.05 | |
| **Ig** | $(CH_2)_5CH_3$ | $(CH_2)_5CH_3$ | H | H | H | H | 1.4±0.2 | 10% |
| **18** | $(CH_2)_5CH_3$ | $(CH_2)_5CH_3$ | H | $CH_3$ | H | H | 0.299±0.05 | |
| **Ih** | $CH(CH_3)_2$ | $CH(CH_3)_2$ | H | H | H | H | 103±9.0 | |

| | | | | | | | | |
|---|---|---|---|---|---|---|---|---|
| **19** | $CH(CH_3)_2$ | $CH(CH_3)_2$ | H | $CH_3$ | H | H | 64.89±5.2 | |
| **Ij** | $CH_2CH_3$ | $CH_2C_6H_5$ | H | H | H | H | 11.0±1.0 | |
| **20** | $CH_2CH_3$ | $CH_2C_6H_5$ | H | $CH_3$ | H | H | 2.92±0.3 | |
| **In** | $(CH_2)_2CH_3$ | $(CH_2)_2CH_3$ | F | H | H | H | 4.28±0.32 | 4.3% |
| **21** | $(CH_2)_2CH_3$ | $(CH_2)_2CH_3$ | F | $CH_3$ | H | H | 19.80±2.0 | |
| **Ip** | $(CH_2)_5CH_3$ | $(CH_2)_5CH_3$ | F | H | H | H | 0.37±0.13 | 0% |
| **22** | $(CH_2)_5CH_3$ | $(CH_2)_5CH_3$ | F | $CH_3$ | H | H | 1.07±0.11 | |
| **Iv** | $(CH_2)_2CH_3$ | $(CH_2)_2CH_3$ | $NO_2$ | H | H | H | 0.95±0.1 | |
| **23** | $(CH_2)_2CH_3$ | $(CH_2)_2CH_3$ | $NO_2$ | $CH_3$ | H | H | 5.70±0.45 | |
| **Isss** | $CH_3$ | $(CH_2)_3CH_3$ | H | H | H | H | 53.3±4.0 | |
| **24** | $CH_3$ | $(CH_2)_3CH_3$ | H | $CH_3$ | H | H | 190.0±10 | |
| **Ittt** | $CH_3$ | $(CH_2)_4CH_3$ | H | H | H | H | 12.1±1.0 | |
| **25** | $CH_3$ | $(CH_2)_4CH_3$ | H | $CH_3$ | H | H | 38.16±4.0 | |
| **Iuuu** | $CH_2CH_3$ | $(CH_2)_3CH_3$ | H | H | H | H | 12.6±1.0 | |
| **26** | $CH_2CH_3$ | $(CH_2)_3CH_3$ | H | $CH_3$ | H | H | 60.24±6.0 | |
| **Izzz** | $CH_3$ | $CH_2C_6H_5$ | H | H | H | H | 12.0±1.0 | |
| **27** | $CH_3$ | $CH_2C_6H_5$ | H | $CH_3$ | H | H | 20.93±1.8 | |
| **Iaab** | $CH_3$ | $CH_2C_6H_5$ | F | H | H | H | 1.8±0.1 | |

[a] The concentration of tested compounds that inhibited [$^3$H]PK 11195 binding to rat kidney mitochondrial membranes ($IC_{50}$) by 50% was determined with six concentrations of the displacers, each performed in triplicate. K*i* values are the mean ± SEM of three determinations. [b] The inhibition percent of [$^3$H]flumazenil specific binding at 10 μM of the compound are the mean ± SEM of five determinations. K*i* values are the mean ± SEM of three determinations. [c] Data taken from ref. 39

# Introduction to Experimental Section

*N,N*-dialkyl-2-phenylindol-3-ylglyoxylamide derivatives, designed in 2004 by Primofiore et al.[37], have shown a high affinity for TSPO in the nanomolar to subnanomolar range and a high selectivity for TSPO. The same research group has successively refined the TSPO pharmacophore/topological model through the synthesis and the biological evaluation of a library of novel 2-phenylindol-3- ylglyoxylamide derivatives of general formula (**I**).[34]

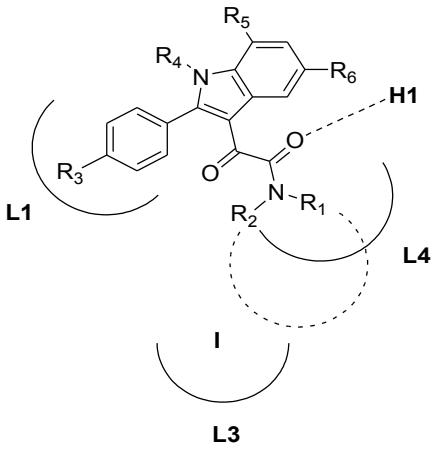


**Figura 14.** N,N-dialkyl-2-phenylindol-3-ylglyoxylamides

As earlier mentioned, rationalizing the SARs in the light of the previously reported pharmacophore/receptor model made up of three lipophilic pockets (L1, L3, L4) and an H-bond donor group (H1), these authors have individuated four fundamental interactions: [5, 39]

1. the second carbonyl group of the oxalyl bridge engages an H-bond with the donor site H1;

2. the two lipophilic substituents $R_1$ and $R_2$ (linear or ramified alkyl, arylalkyl group) on the amide nitrogen interact hydrophobically with the L3 or L4 lipophilic pockets;

3. the 2-phenyl group establishes π-stacking interactions within the L1 pocket.

Taking into account these observations, the aim of this work is to refine the TSPO pharmacophore/topological model through the synthesis and biological evaluation of a series of *N,N*-dialkyl-2-phenylindol-3-ylglyoxylamides (**II**) bearing a polar group at the 4'-position of the 2-phenyl ring ($R_3$ = $NH_2$, OH, COOH), and of a series of *N,N*-dialkyl-2-(3-thienyl)indol-3-ylglyoxylamides (**III**). These compounds have been synthesized as symmetrical amides featuring linear alkyl chains on the amide nitrogen (in particular *n*-propyl) to evaluate any changes in the interaction with the lipophilic pockets L3, L4 of the pharmacophore. The TSPO affinity of intermediary compounds featuring a $OCH_3$ and a $COOCH_3$ substituent in 4'-position has also been estimated.

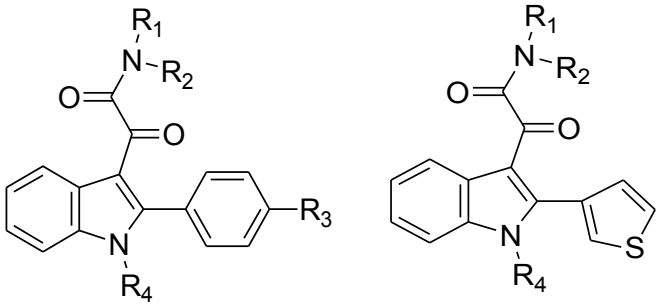

**II** **III**

**Figure 15.** General structures of *N,N*-dialkyl-2-phenylindol-3-ylglyoxylamides (**II**) and *N,N*-dialkyl-2-(3-thienyl)indol-3-ylglyoxylamides (**III**).

The basal expression of TSPO is up-regulated in a number of neuropathologies, including gliomas and neurodegenerative diseases, in various forms of brain injury and inflammation, as well as in a variety of tumors.
So, for this reasons, TSPO has been suggested as a promising diagnostic marker to image and measure the TSPO expression and distribution levels, and thus for evaluation of disease progression by means of specific fluorescent or radiolabeled ligands. In particular, PET imaging using TSPO ligands to label activated microglia offers quantitative measures of inflammation, and then can help to understand the regional brain distribution, stage and severity of neuroinflammation.
Evaluating a novel series of 2-phenylindol-3-ylglyoxylamides featuring a methyl substituent on the indole nitrogen the same research group, in collaboration with Pike and coworkers [39], has observed that the insertion of the methyl group at the $N^1$-position does not significantly influence TSPO binding, according with the pharmacophore model proposed. Therefore, these authors have developed novel radioligands for imaging brain TSPO with PET labeling the indole at the $N^1$-position with the positron emitter carbon-11, and have indicated these compounds as promising new chemotype for development of novel TSPO radioligands as biomarkers of neuroinflammation.
Therefore, the choice to insert a polar group in the scaffold of indolylglyoxylamide derivatives has been made with the purpose to improve the lipophilic/hydrophilic balance, envisaging the possibility to develop novel TSPO radioligands with a better pharmacokinetic profile. In fact, it has been previously observed that highly lipophilic molecular probes show a high level of non-specific binding and thus a poor signal-to-noise ratios, a high plasma protein binding and thus a relatively poor penetration of the blood-brain barrier, which results in a low levels of tracer accumulation in brain.[43]
At the same time, it has also been evaluated the influence on the TSPO binding of the insertion of the methyl group at the $N^1$-position: $N^1$-methylated indoles have been prepared and their K*i* values compared with those of the $N^1$-unsubstitued parent compounds and the standard TSPO ligands Ro 5-4864 (**2**), PK11195 (**5**) and alpidem (**6**).

In this thesis work it has been prepared and evaluated the compounds **38** (2-(3-thienyl)), **40** ($R_3 = NH_2$), **42** ($R_3$ = OH), **44** ($R_3$ = COOH), methylated at the $N^1$-position, and the corresponding $N_1$-unmethylated **37** (2-(3-thienyl)), **39** ($R_3 = NH_2$), **41** ($R_3$ = OH), **43** ($R_3$ = COOH). It has also been estimated the K*i* value of the intermediary $N^1$-unmethylated com-

pounds **31** ($R_3$ = OMe), **32** ($R_3$ = COOMe), and of the corresponding methylated **33** ($R_3$ = OMe), **34** ($R_3$ = COOMe).

The general synthetic procedures employed to prepare these compounds are shown in **Scheme 1** and **2.** They involve, as first step, the synthesis of the 2-phenylindoles **29a-c** and 2-(3-thienyl)indole **35** through a one-step Fischer indole synthesis[34] consisting in warming phenylhydrazine hydrochloride and the appropriate acetophenone, or methyl 4-acetylbenzoate, or acetylthiophene directly with an excess of acid catalyst PPA (polyphosphoric acid). The reaction mixture was then poured into ice and the precipitated solid was collected by filtration and purified by recrystallization from toluene.

The indoles **29a-c** and **35** were then acylated with oxalyl chloride in anhydrous ethyl ether at 0 °C to give the corresponding indolylglyoxylyl chlorides **30a-c** and **36**, which were allowed to react in dry toluene solution and nitrogen atmosphere with dipropilammine in presence of triethylamine, in equimolar quantity so as neutralize the hydrochloridric acid formed during the reaction of condensation.[37] The crude compounds, after washing with a solution of $NaHCO_3$ dil. 5% and then with $H_2O$ to eliminate the amine not reacted, with HCl dil. 10% and again $H_2O$ to remove the excess of $Et_3N$, were tritured at 0 °C with ethylic ether to yield the indolylglyoxylamides **1v**, **31-32**, and **37.**

These compounds were then methylated at the $N^1$-position through the treatment with sodium hydride and subsequent addition of an excess of methyl iodide in dry DMF.[39] The reaction mixture was dripped into ice and the solid precipitated was collected by filtration, dried and subsequently purified by recrystallization from toluene to obtained the $N^1$-methylated indolylglyoxylamides **23**, **33-34**, and **38**. Their chemical-physical properties were determined, and their structures were confirmed by $^1$H-NMR [data reported in **Table 4** for compounds **31** and **33** ($R_3$ = OMe), **32**, and **34** ($R_3$ = COOMe), **Table 5** for **37-38** (2-(3-thienyl)), data of compounds **1v** and **23** ($R_1 = R_2 = (CH_2)_2CH_3$; $R_3 = NO_2$) are reported in literature[34]]

**Scheme 1**

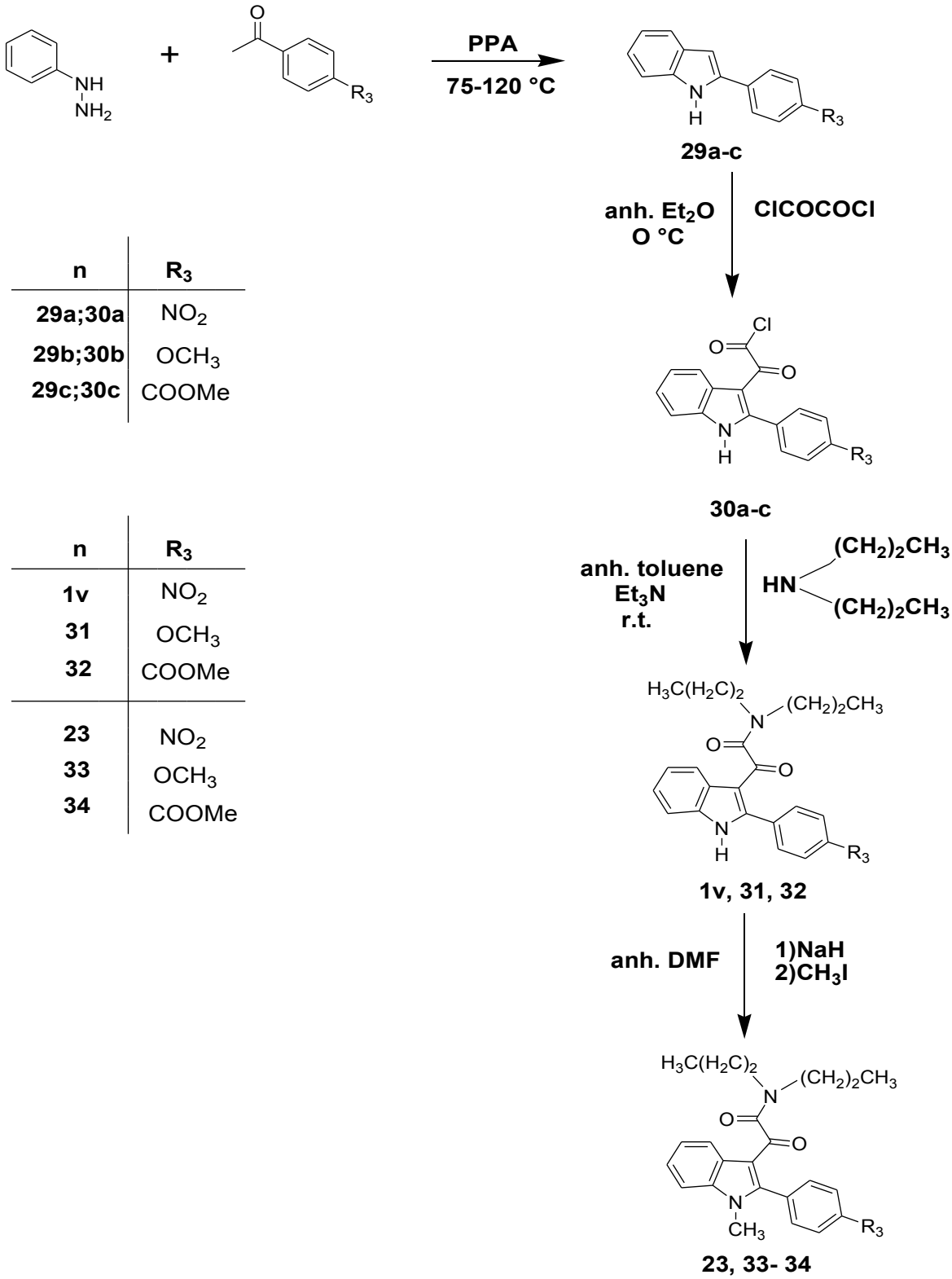


| n | $R_3$ |
|---|---|
| **29a;30a** | $NO_2$ |
| **29b;30b** | $OCH_3$ |
| **29c;30c** | COOMe |

| n | $R_3$ |
|---|---|
| **1v** | $NO_2$ |
| **31** | $OCH_3$ |
| **32** | COOMe |
| **23** | $NO_2$ |
| **33** | $OCH_3$ |
| **34** | COOMe |

**Scheme 2**

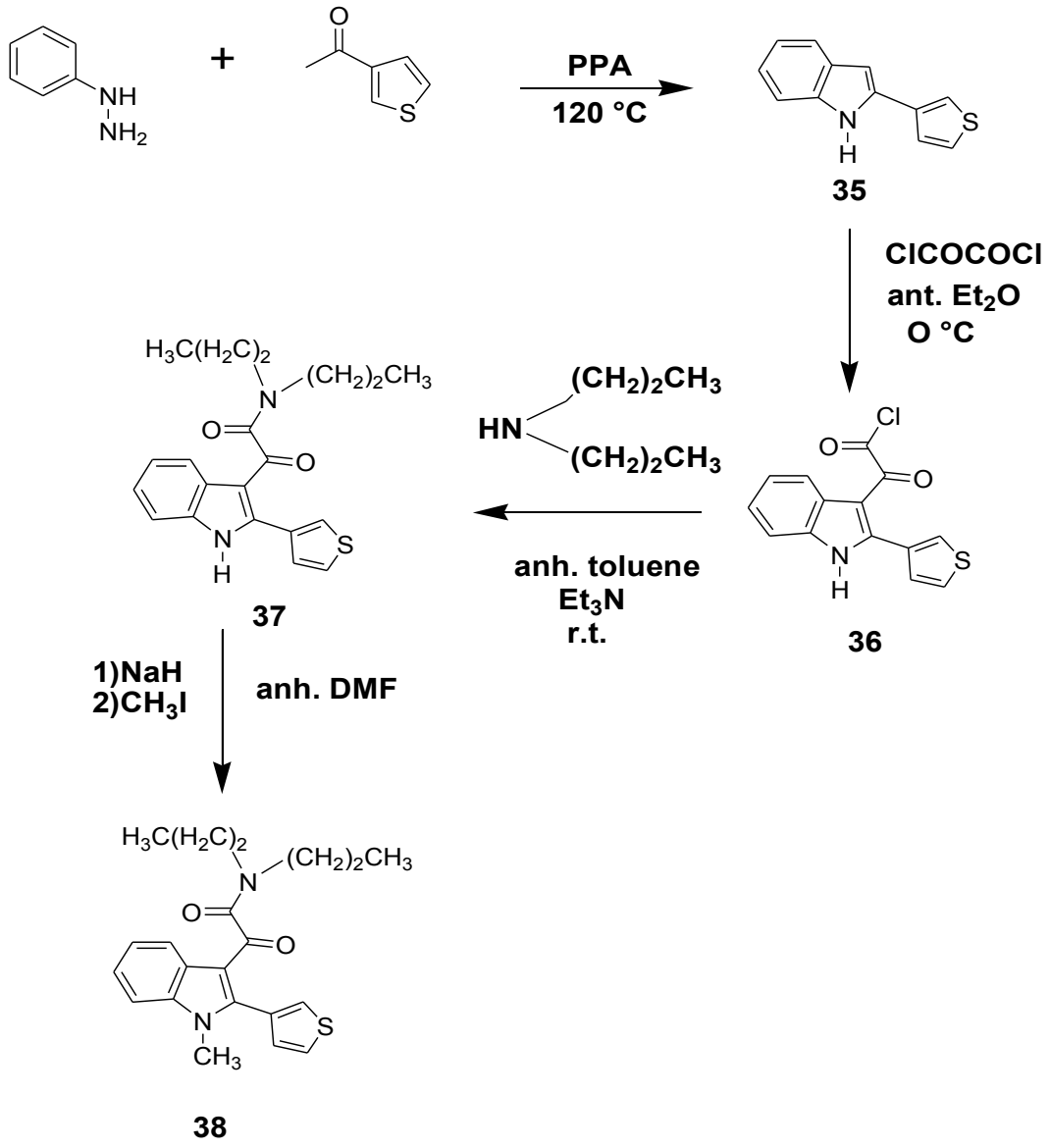


The synthesis of the target compounds **39** ($R_3 = NH_2$), **41** ($R_3 = OH$), and **43** ($R_3 = COOH$) was achieved by the procedures outlined in **Schemes 3**, **4** and **5**. Starting by the $N^1$-methylated (**23**, **33**, **34**) and their parent unmethylated (**1v**, **31** ,**32** ) indoles, previously prepared, we obtain, through appropriate reactions, the corresponding compounds featuring a polar group at the 4'-position of the 2-phenyl ring.

**Scheme 3**

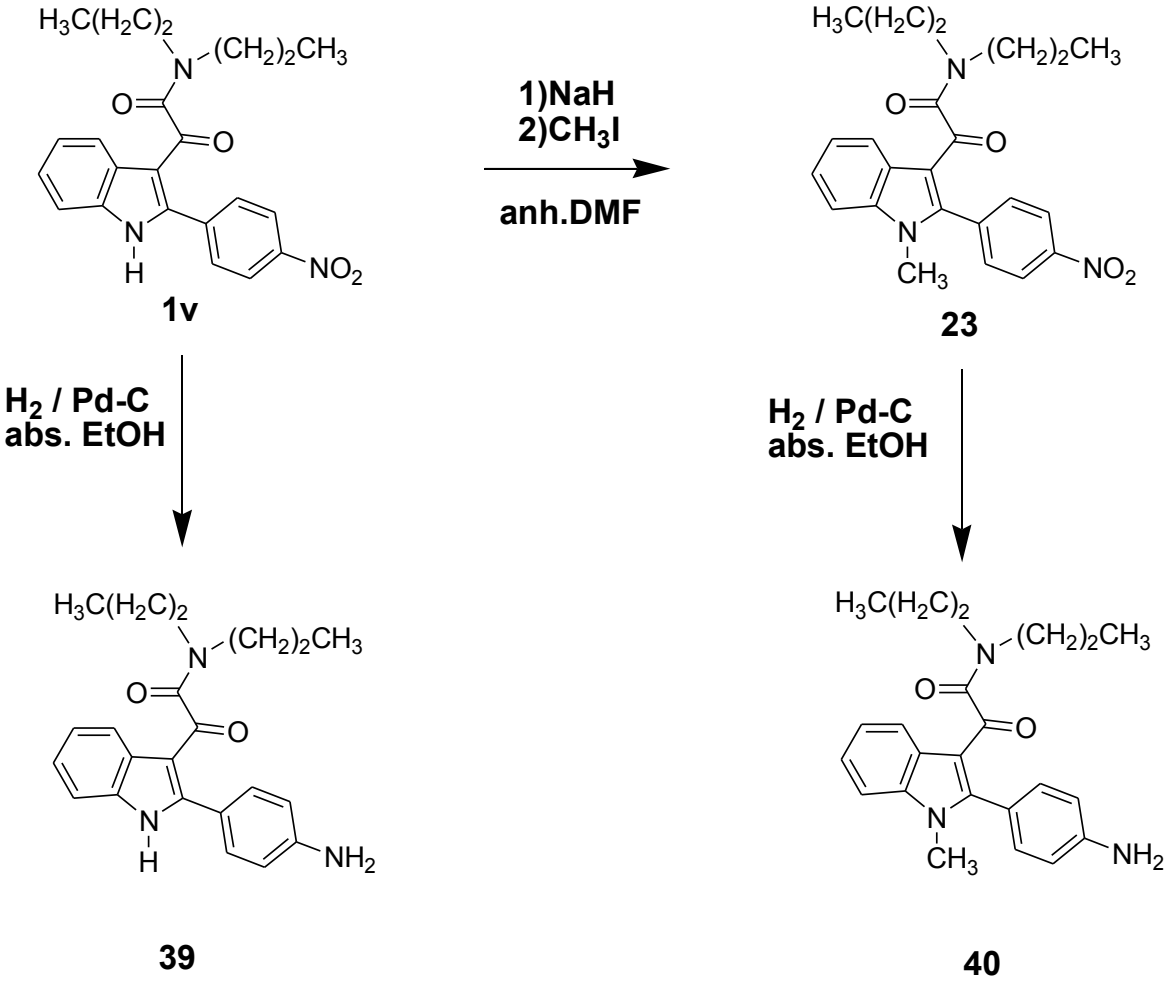


**The Scheme 3**, reported above, describes the general procedure for the synthesis of the 2-phenylindolylglyolamide derivatives bearing a $NH_2$ in *para* position at the 2-phenyl ring:[41] *N,N*-dialkyl-[2-(4-nitrophenyl)indol-3-yl]glyoxylamide derivatives **1v** and **23** were catalytically hydrogenated over palladium to yield the relative amines **39** and **40**. Their chemical-physical properties and $^1$H-NMR data are reported in **Table 6.**

**Scheme 4**

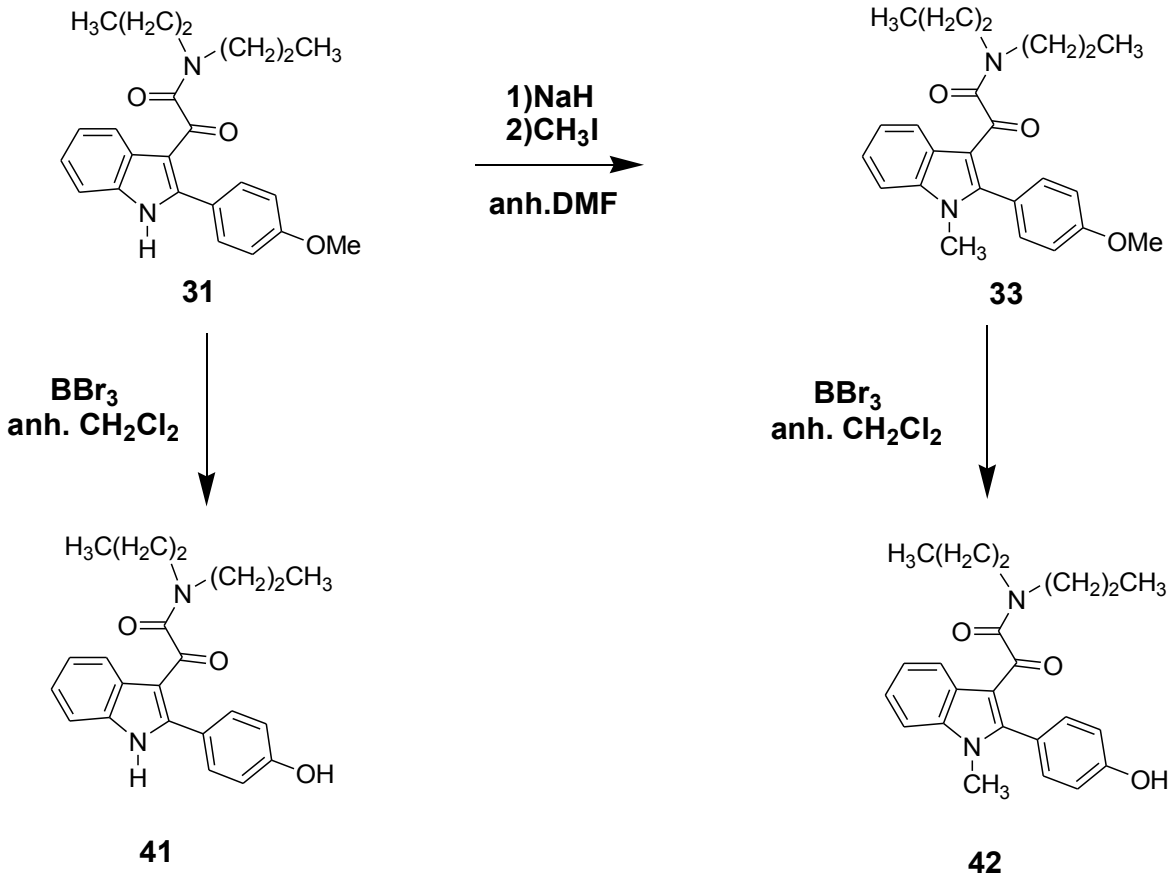


**31** **33** **41** **42**

The phenylindolylglyoxylamide derivatives featuring a OH group in $R_3$ **(41, 42**) were achieved through a demethylation of the methoxy group[47] (**Scheme 4**) in *para* position of the 2-phenyl ring with $BBr_3$, added dropwise in nitrogen atmosphere to a stirred suspension of derivatives **31** or **33**. Finally, methanol was added to the reaction mixture to hydrolyze the excess of $BBr_3$, and crude compounds were recovered as a solid precipitated after evaporation under reduced pressure. Their chemical-physical properties and $^1$H-NMR data are reported in **Table 6.**

Instead, the **Scheme 5** reported the synthetic procedure to obtain compounds **43-44** by hydrolysis of the methyl ester[48] in *para* position adding lithium hydroxide monohydrate to a MeOH/$H_2O$ (3:1) solution of methyl derivatives **32** or **34**. Their chemical-physical properties and $^1$H-NMR data are reported in **Table 6.**

**Scheme 5**

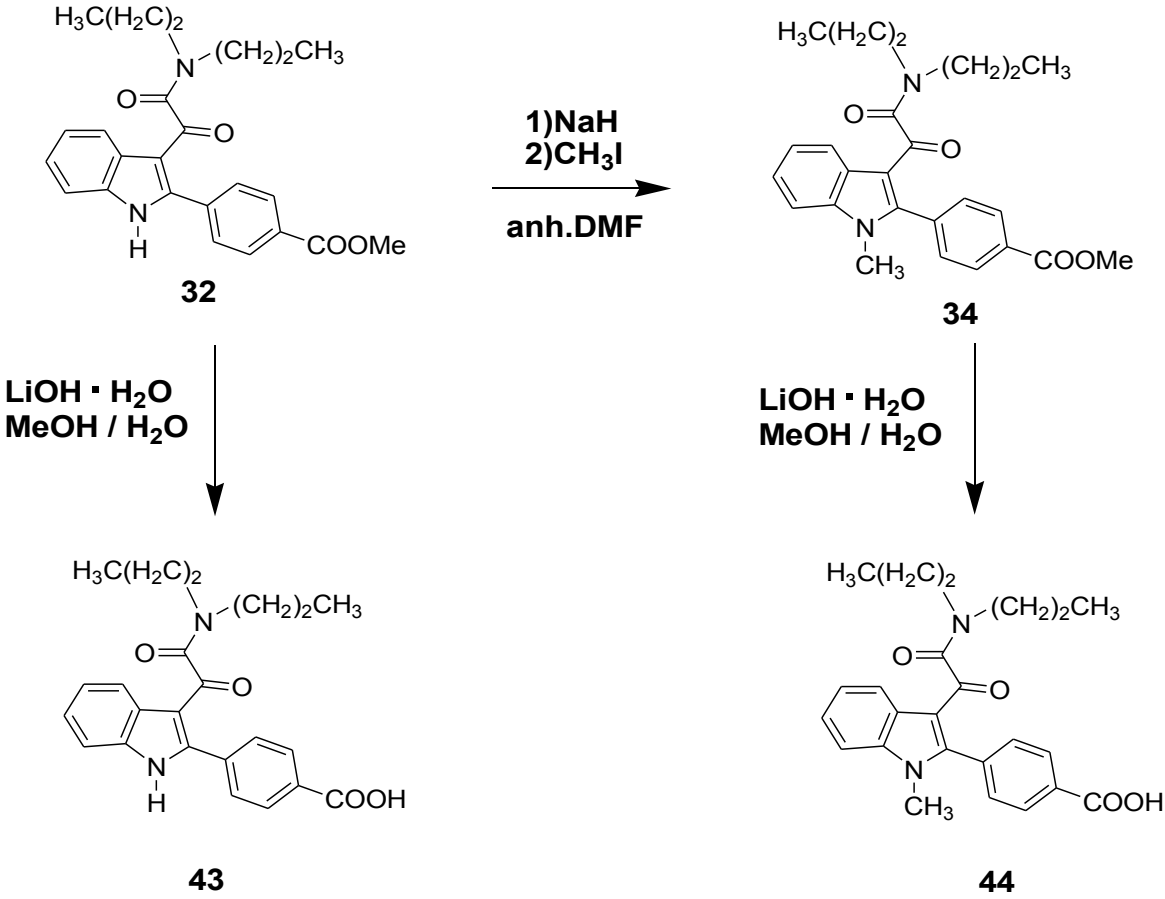


**32** **34** **43** **44**

**Table 4.** Yields, melting points, and spectral data of compounds **31, 32, 33** and **34.**

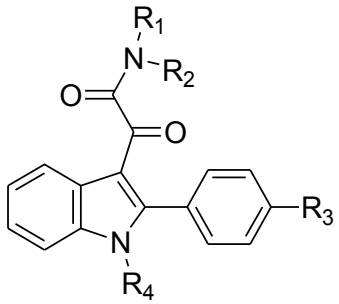


| n | $R_1 = R_2$ | $R_3$ | $R_4$ | yield (%) | m.p. (°C) *(recryst. solvent)* | $^1$H-NMR (DMSO-$d_6$, ppm) | formula |
|---|---|---|---|---|---|---|---|
| **31** | $(CH_2)_2CH_3$ | $OCH_3$ | H | 52 | 121-126 *(toluene)* | 0.64-0.79 ( m, 6H, $CH_2CH_2\underline{CH_3}$); 1.21-1.26 ( m, 2H, $CH_2\underline{CH_2}CH_3$); 1.39-1.47 ( m, 2H, $CH_2\underline{CH_2}CH_3$); 2.93-3.06 ( 2t, 4H, J=7Hz, $\underline{CH_2}CH_2CH_3$); 3.83 ( s, 3H, $OCH_3$); 7.06 (d, 2H, J=8 Hz, ArH); 7.08-7.29 (m, 2H, ArH); 7.42 (d, 1H, J=8 Hz, ArH); 7.50 (d, 2H, J=8 Hz, ArH); 8.01 (d, 1H, J=8 Hz, ArH); 12.34 (s, 1H, NH exch. with $D_2O$). | $C_{23}H_{26}N_2O_3$ |

| n | $R_1 = R_2$ | $R_3$ | $R_4$ | yield (%) | m.p. (°C) *(recryst. solvent)* | $^1$H-NMR (DMSO-$d_6$, ppm) | formula |
|---|---|---|---|---|---|---|---|
| **32** | $(CH_2)_2CH_3$ | $COOCH_3$ | H | 65 | 139-141 *(toluene)* | 0.66-0.77 ( m, 6H, $CH_2CH_2\underline{CH_3}$); 1.20-1.27 ( m ,2H, $CH_2\underline{CH_2}CH_3$); 1.45-1.49 ( m, 2H ,$CH_2\underline{CH_2}CH_3$); 2.93-3.10 ( 2t, 4H, J=8Hz, $\underline{CH_2}CH_2CH_3$); 3.92 (1s, 3H, $COOCH_3$); 7.27-7.31 (m, 2H, ArH); 7.52 (d, 1H, J=8 Hz, ArH); 7.74 (d, 2H, J=8 Hz, ArH);8.02-8.09 (m, 3H, ArH); 12.64 (s, 1H, NH exch. with $D_2O$). | $C_{24}H_{26}N_2O_4$ |
| **33** | $(CH_2)_2CH_3$ | $OCH_3$ | $CH_3$ | 69 | 135-137 *(toluene)* | 0.67-0.75 (m, 6H, $CH_2CH_2\underline{CH_3}$); 1.03-1.14 (m, 2H, $CH_2\underline{CH_2}CH_3$); 1.41-1.52 (m, 2H, $CH_2\underline{CH_2}CH_3$); 2.71-2.97 (2t, 4H, J=7 Hz, $\underline{CH_2}CH_2CH_3$); 3.50 (s, 3H, $NCH_3$); 3.84 (s, 3H, $OCH_3$);7.07 (d, 2H, J=8 Hz, ArH); 7.32-7.39 (m, 4H, ArH); 7.63 (d, 1H, J=8 Hz, ArH); 8.21(d, 1H, J=8,ArH). | $C_{24}H_{28}N_2O_3$ |

| | | | | | | | |
|---|---|---|---|---|---|---|---|
| **34** | $(CH_2)_2CH_3$ | $COOCH_3$ | $CH_3$ | 56 | 135-137<br>*(toluene)* | 0.64-0.75 (m, 6H, $CH_2CH_2\underline{CH_3}$); 1.03-1.07 (m, 2H, $CH_2\underline{CH_2}CH_3$); 1.37-1.60 (m, 2H, $CH_2\underline{CH_2}CH_3$); 2.73-2.98 (2t, 4H, J=8 Hz, $\underline{CH_2}CH_2CH_3$); 3.52 (s, 3H, $NCH_3$); 3.92 (s, 3H, $COOCH_3$); 7.25-7.42 (m, 2H, ArH); 7.61-7.65 (m, 3H, ArH); 8.06-8.20 (m, 3H, ArH). | $C_{25}H_{28}N_2O_4$ |

**Table 5.** Yields, melting points, and spectral data of compounds **37, 38.**

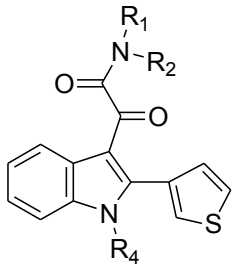


| n | $R_1 = R_2$ | $R_4$ | yield (%) | m.p. (°C) *(recryst. solvent)* | $^1$H-NMR (DMSO-$d_6$, ppm) | formula |
|---|---|---|---|---|---|---|
| **37** | $(CH_2)_2CH_3$ | H | 78 | 68-71 | 0.65 (t, 3H, J=8 Hz, $CH_2CH_2\underline{CH_3}$); 0.81 (t, 3H, J=8 Hz, $CH_2CH_2\underline{CH_3}$); 1.30-1.50 (m, 4H, $CH_2\underline{CH_2}CH_3$); 3.00-3.14 (m, 4H, $\underline{CH_2}CH_2CH_3$); 7.21-7.27 (m, 2H, ArH); 7.46-7.50 (m, 2H, ArH); 7.69-7.73 (m, 1H, ArH); 7.91 (d, 1H, J=7 Hz, ArH); 8.13 (d, 1H, J=2 Hz, ArH); 12.45 (s, 1H, NH exch. with $D_2O$). | $C_{20}H_{22}N_2O_2S$ |
| **38** | $(CH_2)_2CH_3$ | $CH_3$ | 65 | 118-121 | 0.67-0.81 (m, 6H, $CH_2CH_2CH_3$); 1.24-1.48 (m, 4H, $CH_2CH_2CH_3$); 2.80-3.00 (2t, 4H, J=8 Hz, $CH_2CH_2CH_3$); 3.54 (s, 3H, $NCH_3$); 7.24 (d, 1H, J=7 Hz, ArH); 7.32-7.38 (m, 2H, ArH); 7.65 (d, 1H, J=7 Hz, ArH); 7.72-7.79 (m, 2H, ArH); 8.21 (d, 1H, J=7 Hz, ArH). | $C_{21}H_{24}N_2O_2S$ |

**Table 6.** Yields, melting points, and spectral data of compounds **39-44**.

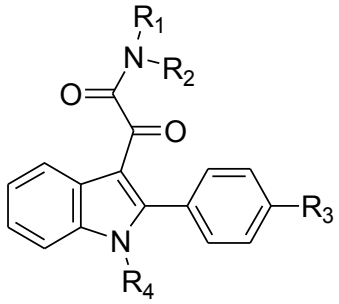


| n | $R_1 = R_2$ | $R_3$ | $R_4$ | yield (%) | m.p. (°C) *(recryst. solvent)* | $^1$H-NMR (DMSO-$d_6$, ppm) | formula |
|---|---|---|---|---|---|---|---|
| **39** | $(CH_2)_2CH_3$ | $NH_2$ | H | 52 | 197-198 *(toluene)* | 0.63-0.84 (m, 6H, $CH_2CH_2\underline{CH_3}$); 1.29-1.37 (m, 2H, $CH_2\underline{CH_2}CH_3$); 1.41-1.49 (m, 2H, $CH_2\underline{CH_2}CH_3$); 2.97- 3.08 (2t, 4H, J=7 Hz, $\underline{CH_2}CH_2CH_3$); 5.57 (s, 2H, $NH_2$ exch. with $D_2O$); 6.62 (d, 2H, J=8 Hz, ArH); 7.17-7.43 (m, 5H, ArH); 7.92-7.97 (m, 1H, ArH); 12.09 (s, 1H, NH exch. with $D_2O$). | $C_{22}H_{25}N_3O_2$ |

| n | $R_1 = R_2$ | $R_3$ | $R_4$ | yield (%) | m.p. (°C) *(recryst. solvent)* | $^1$H-NMR (DMSO-$d_6$, ppm) | formula |
|---|---|---|---|---|---|---|---|
| **40** | $(CH_2)_2CH_3$ | $NH_2$ | $CH_3$ | 82 | 178-180 *(toluene)* | 0.67-0.77 (m, 6H, $CH_2CH_2\underline{CH_3}$); 1.12-1.23 (m, 2H, $CH_2\underline{CH_2}CH_3$); 1.40-1.51 (m, 2H, $CH_2\underline{CH_2}CH_3$); 2.72- 2.97 (2t, 4H, J=8 Hz, $\underline{CH_2}CH_2CH_3$); 3.51 (s, 3H, $NCH_3$); 7.16-7.33 (m, 6H, ArH); 7.59 (d, 1H, J=8 Hz, ArH); 8.19 (d, 1H, J=8 Hz, ArH); 8.56 (d, 2H, J=20 Hz, $NH_2$ exch. with $D_2O$); | $C_{23}H_{27}N_3O_2$ |
| **41** | $(CH_2)_2CH_3$ | OH | H | 59 | 210-212 *(toluene)* | 0.64-0.82 (m, 6H, $CH_2CH_2\underline{CH_3}$); 1.27-1.46 (m, 4H, $CH_2\underline{CH_2}CH_3$); 2.95-3.02 (2t, 4H, J=8 Hz, $\underline{CH_2}CH_2CH_3$); 6.86 (d, 2H, J=8 Hz, ArH); 7.17-7.25 (m, 2H, ArH); 7.40 (d, 3H, J=8 Hz, ArH); 8.01 (d, 1H, J=7 Hz, ArH); 9.89 (s, 1H, OH exch. with $D_2O$); 12.27 (s, 1H, NH exch. with $D_2O$). | $C_{22}H_{24}N_2O_3$ |

| n | $R_1 = R_2$ | $R_3$ | $R_4$ | yield (%) | m.p. (°C) *(recryst. solvent)* | $^1$H-NMR (DMSO-$d_6$, ppm) | formula |
|---|---|---|---|---|---|---|---|
| **42** | $(CH_2)_2CH_3$ | OH | $CH_3$ | 75 | 211-214 | 0.67-0.77 (m, 6H, $CH_2CH_2\underline{CH_3}$); 1.09-1.21 (m, 2H, $CH_2\underline{CH_2}CH_3$); 1.41-1.52 (m, 2H, $CH_2\underline{CH_2}CH_3$); 2.72-2.96 (2t, 4H, J=8 Hz, $\underline{CH_2}CH_2CH_3$); 3.50 (s, 3H, $NCH_3$); 6.88 (d, 2H, J=8 Hz, ArH); 7.23 (d, 2H, J=8 Hz, ArH); 7.33-7.36 (m, 2H, ArH); 7.62 (d, 1H, J=8 Hz, ArH); 8.21 (d, 1H, J=8 Hz, ArH); 9.88 (s, 1H, OH exch. with $D_2O$). | $C_{23}H_{26}N_2O_3$ |
| **43** | $(CH_2)_2CH_3$ | COOH | H | 85 | 292-294 | 0.64-0.75 (m, 6H, $CH_2CH_2\underline{CH_3}$); 1.15-1.26 (m, 2H, $CH_2\underline{CH_2}CH_3$); 1.43-1.47 (m, 2H, $CH_2\underline{CH_2}CH_3$); 2.88-3.15 (2t, 4H, J=8 Hz, $\underline{CH_2}CH_2CH_3$); 7.27-7.31 (m, 2H, ArH); 7.51 (d, 1H, J=8 Hz, ArH); 7.71 (d, 2H, J=8 Hz, ArH); 8.04 (d, 3H, J=8 Hz, ArH); 12.63 (s, 1H, NH exch. with $D_2O$). | $C_{23}H_{24}N_2O_4$ |

| n | $R_1 = R_2$ | $R_3$ | $R_4$ | yield (%) | m.p. (°C) *(recryst. solvent)* | $^1$H-NMR (DMSO-$d_6$, ppm) | formula |
|---|---|---|---|---|---|---|---|
| **44** | $(CH_2)_2CH_3$ | COOH | $CH_3$ | 68 | 287-290 | 0.68-0.72 (m, 6H, $CH_2CH_2\underline{CH_3}$); 0.95-1.20 (m, 2H, $CH_2\underline{CH_2}CH_3$); 1.37-1.61 (m, 2H, $CH_2\underline{CH_2}CH_3$); 2.70-3.11 (2t, 4H, J=8Hz, $\underline{CH_2}CH_2CH_3$); 3.37 (s, 3H, $NCH_3$); 7.28-7.45 (m, 2H, ArH); 7.61 (d, 2H, J=8 Hz, ArH); 7.72 (d, 1H, J=8 Hz, ArH); 8.08 (d, 2H, J=8 Hz, ArH); 8.20 (d, 1H, J=8 Hz, ArH). | $C_{24}H_{26}N_2O$ |

# Biological Studies

All products synthesized during this thesis work were assayed by the research group of Prof. Claudia Martini, Department of Pharmacy, University of Pisa.

The binding affinity at TSPO of all the newly synthesized compounds **37-44** was determined in rat kidney membranes by binding competitions experiments against [$^3$H]PK 11195 as radioligand.[37] For binding studies, crude mitochondrial membranes were incubated with [$^3$H]PK11195 (0.6 nM) in the presence of the test compound in the concentration range (0.05 nM-10 μM) in Tris-HCl buffer (50 mM, pH 7.4), as described in literature. [37] For the active compounds, the $IC_{50}$ values were determined and K*i* values were derived according to the Cheng-Prusoff equation. [49]

**Tables 7** and **8** reports the TSPO binding affinity data expressed as K*i* values (nM), of a number of compounds synthesized in this thesis work, together with the K*i* values of the standard Ro 5-4864 (**2**), PK11195 (**5**), and alpidem (**6**), and of the reference compounds **1d** and **16**.
It should be noted that all compounds show good to high affinity for TSPO, with K*i* values in the nanomolar range.
Analysis of these preliminary data allowed to make few main considerations:

1) The insertion of a methoxy group at the 4'-position of **Id** yields compound **31** showing a slight increase in TSPO affinity (**Id** K*i* = 12.2 nm, **31** K*i*= 5.82 nM).

2) The insertion of hydrophilic substituents (OH, $NH_2$, COOH) on the 2-phenyl ring (compounds **39**, **41**, and **43**) does not determine any significant improvement of the affinity, suggesting the interaction at the level of the $L_1$ pocket is mostly lipophilic. In particular, the insertion of a OH group at the 4'-position of the 2-phenyl ring is tolerated for TSPO affinity (**Id**, K*i* = 12.2 nm, **41** K*i* = 16.13 nM). Conversely, a decrease of the binding affinity is observed introducing a $NH_2$ or, to a major extent, a COOH group (**Id** K*i* = 12.2 nm, **39** K*i* = 44.4 nM, **43** K*i* = 343 nM).

3) The insertion of a lipophilic subsituents ($COOCH_3$, thiophene ring), on the 2-phenyl ring (compound **32** ) shows a low increase in TSPO affinity ( **Id** K*i* = 12.2 nm, **32** K*i* = 3.101 nM), while for compound **37**, shows an elevate increase in TSPO affinity (**37** K*i* = 1.234 nm). Compound **37** results the most potent compound among the products tested.

4) Insertion of a methyl group on the indole $N^1$-nitrogen produces different effects on TSPO affinity in dependence of the substituent at 4'-position. From the comparison of the $N^1$-methyl derivatives with their corresponding $N^1$-unmethylated, the following observations could be drawn:

- the affinity is substantially maintained when the 2-phenyl ring is unsubstituted (**Id** K*i* = 12.2 nm, **16** K*i* = 19.5 nM) or features a 4'-methoxy group (**31** K*i* = 5.82 nm, **33** K*i* = 14.65 nM) or when is present a $COOCH_3$ group (**32** K*i* = 3.101 nm, **34** K*i* = 3.483 nm).

- a significant improvement in TSPO affinity was observed when a $NH_2$ group is present at 4'-position (**39** K*i* = 44.4 nm, **40** K*i* = 5.63 nM), while a decrease was noticed when a thiophene group is present on the 2-indole ring (**37** K*i* = 1.234 nm, **38** K*i* = 21.17 nM).

- the contemporary presence of $N^1$-methyl and 4'-OH moieties yields a detrimental effect on TSPO affinity (**41** K*i* = 16.13 nm, **42** K*i* = 143.3 nM).

- the $N^1$-unmethylated compound (**43**), featuring a 4'-COOH group, presents a low activity and the introduction of the methyl group (**44**) cause the loss of the activity.

Summarizing, it should be speculated that the substitutions at 1'- and 4'-positions seem to significantly modulate TSPO affinity in an interdependent and not additive way.

**Table 7.** Preliminary data of the receptor binding affinity for TSPO.

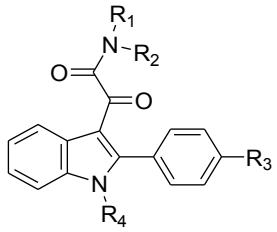

| n | $R_1 = R_2$ | $R_3$ | $R_4$ | TSPO K*i* (nM)[a] |
|---|---|---|---|---|
| **Id** | $(CH_2)_2CH_3$ | H | H | 12.2±1.0 |
| **16** | $(CH_2)_2CH_3$ | H | $CH_3$ | 19.5±1.5 |
| **31** | $(CH_2)_2CH_3$ | $OCH_3$ | H | 5.82±0.5 |
| **33** | $(CH_2)_2CH_3$ | $OCH_3$ | $CH_3$ | 14.65±1.5 |
| **32** | $(CH_2)_2CH_3$ | $COOCH_3$ | H | 3.101±0.3 |
| **34** | $(CH_2)_2CH_3$ | $COOCH_3$ | $CH_3$ | 3.483±0.35 |
| **39** | $(CH_2)_2CH_3$ | $NH_2$ | H | 44.4±5.0 |
| **40** | $(CH_2)_2CH_3$ | $NH_2$ | $CH_3$ | 5.63±0.6 |
| **41** | $(CH_2)_2CH_3$ | OH | H | 16.13±1.0 |
| **42** | $(CH_2)_2CH_3$ | OH | $CH_3$ | 143.3±15 |
| **43** | $(CH_2)_2CH_3$ | COOH | H | 343.0±10 |
| **44** | $(CH_2)_2CH_3$ | COOH | $CH_3$ | Not active |
| **Ro 5-4864** | | | | 23.0±3.0 |
| **PK 11195** | | | | 9.30±0.5 |
| **alpidem** | | | | 0.5 – 7 |

**Table 8** Preliminary data of the receptor binding affinity for TSPO.

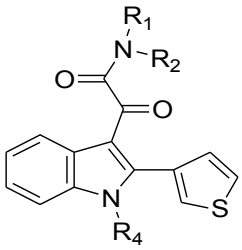


| n | $R_1 = R_2$ | $R_3$ | $R_4$ | TSPO K*i* (nM)[a] |
|---|---|---|---|---|
| **Id** | $(CH_2)_2CH_3$ | H | H | 12.2±1.0 |
| **16** | $(CH_2)_2CH_3$ | H | $CH_3$ | 19.5±1.5 |
| **37** | $(CH_2)_2CH_3$ | thiophene ring | H | 1.234±0.12 |
| **38** | $(CH_2)_2CH_3$ | thiophene ring | $CH_3$ | 21.17±0.2 |
| **Ro 5-4864** | | | | 23.0±3.0 |
| **PK 11195** | | | | 9.30±0.5 |
| **alpidem** | | | | 0.5 – 7 |

[a]The concentration of tested compounds that inhibited [$^3$H]PK 1195 binding to rat kidney mitochondrial membranes ($IC_{50}$) by 50% was determined with six concentrations of the displacers, each performed in triplicate. K*i* values are the mean ±SEM of three determinations.

# Materials and Methods

Melting points were determined using a Reichert Köfler hot-stage apparatus and are uncorrected. Routine nuclear magnetic resonance spectra were recorded in DMSO-$d_6$ solution on a Varian Gemini 200 spectrometer operating at 200 MHz. Evaporation was performed in vacuo (rotary evaporator). Analytical TLC was carried out on Merck 0.2 mm precoated silica gel aluminum sheets (60 F-254). Silica gel 60 Merck (230-400 mesh ASTM) was used for column chromatography. Anhydrous reactions were performed in flame-dried glassware under $N_2$. All compounds showed ≥ 95% purity.

All reagents used were obtained from commercial sources. All solvents were of an analytical grade.

**General procedure for the synthesis of:**

**2-phenyl-1H-indole derivatives (29a, 29b)**
**methyl 4-(1H-indol-2-yl)benzoate derivative (29c)**
**2-(3-thienyl)-1H-indole derivative (35)**

1 g of polyphosphoric acid (PPA) was added to a mixture of phenylhydrazine chlorhydrate (5.0 mmol) and methyl 4-acetylbenzoate (5.0 mmol), or the appropriate acetophenone or acetylthiophene (5.0 mmol). The reaction was maintained at 75°C for 30 min for 29a at 120°C for 4 h for **29b** and **35** and at 60°C for 4 h for compound **29c**. When the starting material was disappeared, the reaction mixture was poured into ice and the precipitated solid was collected by filtration. All products were purified by recrystallization from toluene.
Yield, melting point, and spectral data of compound **29a** were reported in literature.[34]

*2-(4-methoxyphenyl)-1H-indole* (**29b**). Yield: 84%; m. p.: 231-234 °C; $^1$H-NMR (DMSO-$d_6$, ppm): 3.80 (s, 3H, $OCH_3$); 6.76 (d, 1H, J = 1.8 Hz, ArH); 6.96-7.09 (m, 4H, ArH); 7.36 (d, 1H, J = 8 Hz, ArH); 7.49 (d, 1H, J = 7.2 Hz, ArH); 7.77-7.81 (m, 2H, ArH); 11.40 (s, 1H, NH exch. with $D_2O$).

*Methyl 4-(1H-indol-2-yl)benzoate* (**29c**). Yield: 78%; m. p.: 204-207 °C; $^1$H-NMR (DMSO-$d_6$, ppm): 3.87 (s, 3H, $COOCH_3$); 7.02-7.15 (m, 3H, ArH); 7.43 (d, 1H, J=8 Hz, ArH); 7.57 (d, 1H, J=8 Hz, ArH); 8.02 (s, 4H, ArH); 11.73 (s, 1H, NH exch. with $D_2O$).

*2-(3-thienyl)-1H-indole* (**35**). Yield: 89%; m. p.: 243-245 °C; $^1$H-NMR (DMSO-$d_6$, ppm): 6.76 (d, 1H, J = 0.8 Hz, ArH); 6.94-7.12 (m, 2H, ArH); 7.37 (d, 1H, J = 8 Hz, ArH); 7.51 (d, 1H, J = 8 Hz, ArH); 7.59-7.67 (m, 2H, ArH); 7.87 (t, 1H, J = 1.5 Hz, ArH).

**General procedure for the synthesis of:**

**(2-phenylindol-3-yl)glyoxylyl chloride derivatives (30a, 30b)**
**methyl 4-(3-chloroglyoxylylindol-2-yl)benzoate derivative (30c)**
**[2-(3-thienyl)indol-3-yl]glyoxylyl chloride derivative (36)**

Oxalyl chloride (8.0 mmol) was added dropwise at 0°C to a well-stirred mixture of the appropriate indole **29a-c** or **35** (4.0 mmol) in freshly distilled diethyl ether (10 mL). The mixture was maintained at room temperature for 2-24 h (TLC analysis: chloroform). A solid precipitate was obtained in the case of compounds **30b** and **30c**, which was collected by vacuum filtration, and immediately used in the subsequent reaction. Instead, starting by compounds **29a** and **35,** it was not observed any formation of precipitate: thus, the solvent of reaction was evaporated under reduced pressure, and the generated solid was washed with portions of anhydrous diethyl ether to give the correspondent acyl chlorides **30a** and **36.**

[*2-(4-nitrophenyl)indol-3-yl*]*glyoxylyl chloride* **(30a)**. Yield: 60%

[*2-(4-methoxyphenyl)indol-3-yl*]*glyoxylyl chloride* (**30b**). Yield: 72%

*Methyl 4-(3-chloroglyoxylylindol-2-yl)benzoate* (**30c**). Yield: 80%

[*2-(3-thienyl)indol-3-yl*]*glyoxylyl chloride* (**36**). Yield: 65%

**General procedure for the synthesis of:**

**N,N-dialkyl-(2-phenylindol-3-yl)glyoxylamide derivatives (1v, 31)**

**methyl 4-(3-dialkylaminoglyoxylylindole-2-yl)benzoate derivatives (32)**

**N,N-dialkyl-[2-(3-thienyl)indol-3-yl]glyoxylamide derivatives (37)**

A solution of dipropylamine (2.0 mmol) in 5 mL of dry toluene was added dropwise to a stirred suspension, cooled at 0°C, of the (2-phenylindol-3-yl)glyoxylyl chloride derivatives **30a-30b**, or methyl 4-(3-chloroglyoxylylindol-2-yl)benzoate derivative **30c**, or [2-(3-thienyl)indol-3-yl]glyoxylyl chloride derivative **36** (2.0 mmol) in 50 mL of the same solvent, followed by the addition of a solution of triethylamine (2.0 mmol). The reaction mixture was left under stirring for 2-24 h at room temperature (TLC analysis with appropriate eluent), and then filtered. The collected precipitate was triturated with a $NaHCO_3$ 5% aqueous solution, washed with water, and collected again to give a first portion of crude product. The toluene solution was instead removed under reduced pressure, and the oily residue obtained was extracted with $CHCl_3$ and purified by washing with 1) a solution of $NaHCO_3$ dil. 5%; 2) $H_2O$; 3) HCl dil. 10%; and finally 4) $H_2O$. After drying with $MgSO_4$, the chloroform solution was evaporated to dryness, and the residue was tritured at 0 °C with ethylic ether to yield the crude product, that was collected by filtration. In the case of less soluble products, the crude compound precipitates together with the triethylamine hydrochloride and was collected, after washing with a solution of $NaHCO_3$ dil. 5%, and dried over $P_2O_5$ in vacuo.
All products generally did not require additional purification steps, but in the case of dirty compounds they were purified by recrystallization from toluene; only the compound **1v**, N,N-di-n-propyl-[2-(4-nitrophenyl)indol-3-yl]glyoxylamide, was purified by flash chromatography ($CHCl_3$ as eluent), as reported in literature.[34]
Yields, melting points, and spectral data of compounds **31** and **32** are listed in **Table 4**, **37** in **Table 5**, while those of compound **1v** were reported in literature.[34]

**General procedure for the synthesis of:**

**N,N-dialkyl-(N1-methyl-2-phenylindol-3-yl)glyoxylamide derivatives (23, 33)**
**methyl 4-(N1-methyl-3-dialkylaminoglyoxylylindol-2-yl)benzoate derivatives (34)**
**N,N-dialkyl-2-[N1-methyl-(3-thienyl)indol-3-yl]glyoxylamide derivatives (38)**

Sodium hydride (0.2 mmol, 60 % dispersion in mineral oil) was added portionwise, under a nitrogen atmosphere, to an ice-coooled solution of the appropriate N,N-dialkyl-(2-phenylindol-3-yl)glyoxylamide derivatives **1v**, **31**, **32** and **37** in dry DMF (3 mL). Once hydrogen evolution ceased, an excess of methyl iodide (0.6 mmol) was quickly added at 0 °C. The reaction was maintained under stirring at room temperature until the disappearance of starting material (TLC analysis with appropriate eluent). The mixture was then dripped into ice and the solid precipitated was collected by filtration, dried and subsequently purified by recrystallization from toluene. Only the compound **23** was purified by flash chromatography ($CHCl_3$ as eluent). [39]
Yields, melting points, and spectral data of compounds **33** and **34** are listed in **Table 4**, **38** in **Table 5**, while those of compound **23** were reported in literature. [39]

**General procedure for the synthesis of:**
**N,N-dialkyl-[2-(4-aminophenyl)indol-3-yl]glyoxylamide derivatives (39, 40)**

Pd/C 10% (0.05 g) was added to a suspension of the appropriate N,N-dialkyl-[2-(4-aminophenyl)indol-3-yl]glyoxylamide derivatives **1v** or **23** (0.65 mmol) in 150 mL of absolute ethanol. The mixture was hydrogenated under stirring for 5 h at room temperature and reduced pressure. Once hydrogen absorption ceased, the catalyst was filtered off and the ethanolic solution was evaporated to dryness at reduced pressure.
All products were purified by recrystallization from toluene. Yields, melting points, and spectral data of compounds **39** and **40** are listed in **Table 6**.

**General procedure for the synthesis of:**
**N,N-dialkyl-[2-(4-hydroxyphenyl)indol-3-yl]glyoxylamide derivatives (41, 42)**

To a stirred suspension of N,N-dialkyl-[2-(4-methoxyphenyl)indol-3-yl]glyoxylamide derivatives **31**or **33** (0.5 mmol) in 10 mL of dry dichloromethane cooled at -10 °C were added dropwise 0.2 mL of $BBr_3$. The mixture was left under stirring for 30 min. at -10 °C, and subsequently at room temperature for 1h under nitrogen atmosphere. Finally, the solution was cooled again, and was added 5 ml of methanol to hydrolyze the excess of $BBr_3$. The solvent was evaporated at reduced pressure, and the solid precipitate was washed several times with methanol.
The residues obtained were purified by recrystallization from toluene.
Yields, melting points, and spectral data of compounds **41** and **42** are listed in **Table 6**.

**General procedure for the synthesis of:**
**4-(3-dialkylaminoglyoxylylindol-2-yl)benzoic acid derivatives (43, 44)**

Lithium hydroxide monohydrate (0.3 mmol) was added to a suspension of methyl 4-(3-dialkylaminoglyoxylylindol-2-yl)benzoate derivatives **32** or **34** (0.5 mmol) in 20 mL of a MeOH/$H_2O$ (3:1) solution. The mixture was stirred under reflux at 80 °C overnight (TLC analysis with appropriate eluent). Subsequently, the solid precipitate was eliminate through vacuum filtration, and the solution was acidified with HCl dil. 10% to pH 5. The acid precipitated in the solution was collected by filtration and generally did not needed any further purification.
Yields, melting points, and spectral data of compounds **43** and **44** are listed in **Table 6**.

# References


1. Da Settimo, F.; Simorini, F.; Taliani, S.; La Motta, C.; Marini, A. M.; Salerno, S.; Bellandi, M.; Novellino, E.; Greco, G.; Cosimelli, B.; Da Pozzo, E.; Costa, B.; Simola, N.; Morelli, M.; Martini, C.; Anxiolytic-like effects of *N,N*-dialkyl-2-phenyliindol-3ylglyoxylamides by modulation of translocator protein promoting neurosteroid bio-synthesis. *J. Med. Chem.*, **2008**, *51*, 5798-5806

2. Chebib, M.; Johnson; G. GABA-activated ligand gated ion channels: medicinal chemistry and molecular biology. *J. Med. Chem.* **2000**, *43*, 1427-1447

3. Costa, E.; Guidotti; A. Molecular mechanisms in the receptor action of benzodiazepines. *Annu. Rev. Pharmacol. Toxicol.* **1979**, *19*. 531-545

4. Braestrup, C.; Squires; R. Specific benzodiazepine receptors in rat brain characterized by high affinity.[$^3$H]diazepam binding. *Proc. Natl. Acad. Sci. U.S.A.* **1977**, *74*, 3805-3809

5. Taliani, S.; Pugliesi, I.; Da Settimo, F.; Structural requirements to obtain highly potent and selective 18 kDa translocator protein (TSPO) ligands. *Curr. Top. Med. Chem.* **2011**, *11*, 860-886

6. Papadopoulos, V.; Baraldi, M.; Guilarte, T. R.; Knudsen, T. B.; Lacapère, J.; Lindemann, P.; Norenberg, M. D.; Nutt, D.; Weizman, A.; Zhang, M. R.; Gavish, M.; Translocator protein (18 kDa): new nomenclature for the peripheral-type benzodiazepine receptor based on its structure and molecular function. *Trends Pharmacol. Sci.* **2006**, *27*, 402-409

7. Marangos, P. J.; Patel, J.; Boulenger, J.; Clark-Rosenberg, R; Characterization of peripheral-type benzodiazepine binding sites in brain using [$^3$H]Ro 5-4864. *Mol. Pharmacol.* **1982**, 22, 26-32

8. Awad, M; Gavish, M; Binding of [$^3$H]Ro 5-4864 and [$^3$H]PK11195 to cerebral cortex and peripheral tissue of various species: species differences and heterogeneity in peripheral benzodiazepine binding sites. *J. Neurochem*. **1987**, *49*, 1407-1414

9. Braestrup, C.; Nielsen, M.; Squires, R.; Laurberg, S.; Benzodiazepine receptor in brain. *Acta Psychiatr. Scand.* **1978**, *58*, 27-32

10. Anholt, R. R. H.; Pedersen, P. L.; De Souza, E. B.; Snyder, S. H.; The peripheral-type benzodiazepine receptor: localization to the mitochondrial outer membrane. *J. Biol. Chem.* **1986**, *261*, 576-583

11. Culty, M.; Li, H.; Boujrad, N.; Amri, H.; Vidic, B.; Bernassau, J. M.; Reversat, J. L.; Papadopoulos, V.; In vitro studies on the role of the peripheral-type benzodiazepine receptor in steroidogenesis. *J. Steroid. Biochem.* **1999**, *69*, 123-130

**12.** Antkiewicz-Michaluk, L.; Mukhin, A. G.; Guidotti, A.; Krueger, K. E.; Purification and characterization of a protein associated with peripheral-type benzodiazepine binding sites. *J. Biol. Chem.* **1988**, *263*, 17317-17321

**13.** McEnery, M. W.; Snowman, A. M.; Trifiletti, R. R.; Snyder, S. H.; Isolation of the mitochondrial benzodiazepine receptor: association with the voltage-dependent anion channel and the adenine nucleotide carrier. *Proc. Natl. Acad. Sci. USA* **1992**, *89*, 3170-3174

**14.** Casellas P.; Galiegue, S.; Basile, A. S.; Peripheral benzodiazepine receptors and mitochondrial function. *Neurochem. Int.* **2002**, *40*, 475-486

**15.** Papadopoulos, V.; Boujrad, N.; Ikonomovic, M. D.; Ferrara, P.; Vidic, B.; Topography of the Leydig cell mitochondrial peripheral-type benzodiazepine receptor. *Mol. Cell. Endocrinol*. **1994**, *104*, R5-R9

**16.** Scarf, A. M.; Ittner, L. M.; Kassiou, M; The translocator protein (18 kDa): central nervous system disease and drug design. *J. Med. Chem.* **2009**, *52*, 581-592

**17.** Blahos II, J.; Whalin, M. E.; Krueger, K. E.; Identification and purification of a 10-kilodalton protein associated with mitochondrial benzodiazepine receptors. *J. Biol. Chem.* **1995**, *270*, 20285-20291

**18.** Li, H.; Degenhardt, B.; Tobin, D.; Yao, Z. X.; Tasken, K.; Papadopoulos, V.; Identification, localization, and function in steroidogenesis of PAP7: a peripheral-type benzodiazepine receptor- and PKA (RIα)-associated protein. *Mol. Endocrinol.* **2001**, *15*, 2211-2228

**19.** Papadopoulos, V.; Lecanu, R.; Brown, R. C.; Han, Z.; Yao, Z. X.; Peripheral-type benzodiazepine receptor in neurosteroid biosynthesis neuropathology and neurological disorders. *Neuroscience.* **2006**, *138*, 749-756

**20.** Hauet, T.; Yao, Z. X.; Bose, H. S.; Wall, C. T:; Han, Z.; Li, W.; Hales, D. B.; Miller, W. L.; Culty, M.; Papadopoulos, V.; Peripheral-type benzodiazepine receptor-mediated action of steroidogenic acute regulatory protein on cholesterol entry into Leydig cell mitochondria. *Mol. Endocrinol.* **2005**, *19*, 540-554

**21.** Galiègue, S.; Jbilo, O.; Combes, T.; Bribes, E.; Carayon, P.; Le Fur, G.; Casallas, P.; Cloning and Characterization of PRAX-1. *J. Biol. Chem.* **1999**, 274, *2938-2952*

**22.** Batarseh, A.; Papadopoulos, V.; Regulation of translocator protein 18 kDa (TSPO) expression in health and disease states. *Mol. Cell. Endocrinol.* **2010**, *327*, 1-12

**23.** Favreau, F.; Rossard, L.; Zhang, K.; Desurmont, T.; Manguy, E.; Belliard, A.; Fabre, S.; Liu, J.; Han, Z.; Thuillier, R.; Papadopoulos, V.; Hauet, T.; Expression and modulation of translocator protein and its partners by hypoxia reoxygenation or ischemia and reperfusion in porcine renal models. *Am. J. Physiol. Renal Physiol.* **2009**, *297*, F177-F190

**24.** James, M.L.; Selleri, S.; Kassiou, M.; Development Of Ligands for the peripheral benzodiazepine receptor. *Curr. Med. Chem.* **2006**, *13*, 1991-2001

**25.** Halestrap, A. P.; What is mitochondrial permeability transition pore? *J. MolCell. Cardiol*.**, 2009**, *46*, 821-831

**26.** Veenman, L.; Shandalov, Y.; Gavish, M.; VDAC activation by the 18 kDA translocator protein (TSPO), implications for apoptosis. *J. Bioenerg. Biomembr.*, **2008**, *40*, 199-205

**27.** Azarashvili, T.; Grachev, D.; Krestinina, O.; Evtodienko, Y.; Yurkov, I.; Papadopoulos, V:; Reiser, G:; The peripheral-type benzodiazepine receptor is involved in control of $Ca^{2+}$-induced permeability transition pore opening in rat brain mitochondria. *Cell Calcium*, **2007**, *42*, 27-39

**28.** Galiegue, S.; Tinel, N.; Casellas, P.; The peripheral benzodiazepine receptor: a promising therapeutic drug target. *Curr. Med. Chem.*, **2003**, *10*, 1563-1572

**29.** Chelli, B.; Rossi, L.; Da Pozzo, E.; Costa, B.; Spinetti, F.; Rechichi, M.; Salvetti, A.; Lena, A.; Simorini, F.; Vanacore, R.; Scatena, F.; Da Settimo, F.; Gremigni, V.; Martini, C.; PIGA (*N,N*-di-n-butyl-5-chloro-2-(4-chlorophenyl)indol-3-ylglyoxylamide), a new mitochondrial benzodiazepine-receptor ligand, induces apoptosis in C6 glioma cells. *Chem. Bio. Chem*., **2005**, *6*, 1-7

**30.** Denora, N.; Laquintana, V.; Trapani, A.; Lopedota, A.; Latrofa, A.; Gallo, J. M.; Tra-pani, G.; Translocator protein (TSPO) ligand□Ara-C (cytarabine) conjugates as a strategy to deliver antineoplastic drugs and to enhance drug clinical potential. *Mol. Pharm.*, **2010**, *7*, 2255-2269

**31.** Margiotta, N.; Denora, N.; Ostuni, R.; Laquintana, V.; Anderson, A.; Johnson, S. W.; Trapani, G.; Natile, G.; Platinum(II) complexes with bioactive carrier ligands having high affinity for the translocator protein. *J. Med. Chem.*, **2010**, *53*, 5144-5154

**32.** Beurdeley-Thomas, A.; Miccoli, L.; Oudard, S:; Dutrillaux, B.; Poupon, M. F.; The peripheral benzodiazepine receptors: a review. *J. Neurooncol.* **2000**, *46*, 45-56

**33.** Gavish, M.; Bachman, I.; Shoukrun, R:; Katz, Y:; Veenman, L.; Weisimger, G.; Weizman, A.; Enigma of the peripheral benzodiazepine receptor. *Pharmacol. Rev.* **1999**, *51*, 629-650

**34.** Da Settimo, F.; Simorini, F.; Taliani, S.; La Motta, C.; Marini, A. M.; Salerno, S.; Bellandi, M.; Novellino, E.; Greco, G.; Cosimelli, B.; Da Pozzo, E.; Costa, B.; Simola, N.; Morelli, M.; Martini, C.; Anxiolytic-like effects of *N,N*-dialkyl-2-phenyliindol-3ylglyoxylamides by modulation of translocator protein promoting neurosteroid biosynthesis. *J. Med. Chem.*, **2008**, *51*, 5798-5806

**35.** Costa, B; Da Pozzo, E.; Chelli, B.; Simola, N.; Morelli, M.; Luisi, M.; Maccheroni, M.; Taliani, S.; Simorini, F.; Da Settimo, F.; Martini, C.; Anxiolytic properties of a 2-phenylindolglyoxylamide TSPO ligand: stimulation of in vitro neurosteroid production affecting GABAA receptor activity. *Psychoneuroendocrinology*, **2011**, *36*, 463-472

**36.** Chelli, B.; Salvetti, A.; Da Pozzo, E.; Rechichi, M.; Spinetti, F.; Rossi, L.; Costa, B.; Lena, A.; Rainaldi, G.; Scatena, F.; Vanacore, V.; Gremigni, V.; Martini, C.; PK 11195 differentially affects cell survival in human wild-type and 18 kDa Translocator Protein-silenced ADF astrocytoma cells. *J. Cell. Biochem.* **2008**, *105*, 712-723

**37.** Primofiore, G.; Da Settimo, F.; Taliani, S.; Simorini, F.; Patrizi, M.P.; Novellino, E.; Greco, G.; Abignente, E.; Costa, B.; Chelli, B.; Martini, C.; *N,N*-dialkyl-2-phenylindol-3-ylglyoxylamides. A new class of potent and selective ligands at the peripheral benzodiazepine receptor. *J. Med. Chem.*, **2004**, *47*, 1852-1855

**38.** Wadsak, W.; Mitterhauser, M.; Basics and principles of radiopharmaceuticals for PET/CT. *Eur. J. Radiol.*, **2010**, *73*, 461-469

**39.** Pike, V.W.; Taliani, S.; Lohith, T.G.; Owen, D.R.J.; Pugliesi, I.; Da Pozzo, E.; Hong, J.; Zoghbi, S.S.; Gunn, R.N.; Parker, C.A.; Rabiner, E.A.; Fujita, M.; Innis, R.B.; Martini, C.; Da Settimo, F.; Evaluation of novel $N^1$-methyl-2-phenylindol-3-ylglyoxylamides as a new chemotype of 18 kDa Translocator Protein-selective ligand suitable for the development of Positron Emission Tomography radioligands. *J. Med. Chem.*, **2011**, *54*, 366-373

**40.** Taliani, S.; Da Pozzo, E.; Bellandi, M.; Bendinelli, S.; Pugliesi, I.; Simorini, F.; La Motta, C.; Salerno, S.; Marini, A.M.; Da Settimo, F.; Cosimelli, B.; Greco, G.; Novellino, E.; Martini, C.; Novel irreversible fluorescent probes targeting the 18 kDa Translocator Protein: synthesis and biological characterization. *J. Med. Chem.*, **2010**, *53*, 4085-4093

**41.** Badawi, R.D.; Aspects of optimization and quantification in three-dimensional Positron Emission Tomography", University of London, **1998**

**42.** Basu, S.; Kwee, T.C.; Surti, S.; Akin, E.A.; Yoo, D.; Alavi, A.; Fundamentals of PET and PET/CT imaging. *Ann. N. Y. Acad. Sci.*, **2011**, *1228*, 1-18

**43.** Doorduin, J.; de Vries, E.F.J.; Dierckx, R.A.; Klein, H.C.; PET imaging of the peripheral benzodiazepine receptor: monitoring disease progress and therapy response in neurodegenerative disorders. *Curr. Pharm. Design.*, **2008**, *14*, 3297-3315

**44.** Matarrese, M.; Moresco, R.M.; Cappelli, A.; Anzini, M.; Vomero, S.; Simonelli, P.; Verza, E.; Magni, F.; Sudati, F.; Soloviev, D:; Todde, S.; Carpinelli, A.; Kienle, M.G.; Fazio, F.; Labeling and evaluation of N-[$^{11}$C]methylated quinoline-2-carboxamides as potential radioligands for visualization of peripheral benzodiazepine receptors. *J. Med. Chem.*, **2001**, *44*, 579-585

**45.** Zhang, M.R.; Ogawa, M.; Maeda, J.; Ito, T.; Noguchi, J.; Kumata, K.; Okauchi, T.; Su-hara, T.; Suzuki, K.; [2-$^{11}$C]isopropyl-, [1-$^{11}$C]ethyl-, [$^{11}$C]methyl-labeled phenoxy-phenyl acetamide derivatives as Positron Emission Tomography ligands for the peripheral benzodiazepine receptor: radiosynthesis, uptake, and in vivo binding in brain. *J. Med. Chem.*, **2006**, *49*, 2735-2742

**46.** Doorduin, J.; Klein, H.C.; Dierckx, R.A.; James, M.; Kassiou, M.; de Vries, E.F.J.; [$^{11}$C]-DPA-713 and [$^{18}$F]-DPA-714 as new PET tracers for TSPO: a comparison with

[$^{11}$C]-(R)-PK11195 in a rat model of Herpes Encephalitis. *Mol. Imaging. Biol.*, **2009**, *11(6)*, 386-398

**47.** Hammond, M.L.; Zambias, R.A.; Chang, M.N.; Jensen, N.P.; McDonald, J.; Thompson, K.; Boulton, D.A.; Kopka, I.E.; Hand, K.M.; Opas, E.E. et al.; Antioxidant-based inhibitors of leukotriene biosynthesis. The discovery of 6-[1-[2-(hydroxymethyl)phenyl]-1-propen-3-yl]-2,3-dihydro-5-benzofuranol, a potent topical antiinflammatory agent. *J. Med. Chem.*, **1990**, *33*, 908-918

**48.** Corey, E.J.; Székely, I.; Shiner, C.S.; Synthesis of 6,9a-oxido-11a, 15a-dihydroxy-prosta-(E)5, (E)13-dienoic acid, an isomer of PGI2 (vane's PGX). *Tetrahedron Lett.*, **1977**, *18*, 3529-3532

**49.** Cheng, Y.; Prusoff, W.H.; Relationship between constant (K*i*) and the concentration of inhibitor which causes 50% inhibition ($IC_{50}$) of an enzymatic reaction. *Biochem. Pharmacol.,* **1973**, *22*, 3099-3108